OAK RIDGE
NATIONAL LABORATORY
MANAGED BY UT-BATTELLE
FOR THE DEPARTMENT OF ENERGY

ORNL/TM-2008/004

Error Reduction for Weigh-In-Motion

July 25, 2008

Prepared by
L. M. Hively
R. K. Abercrombie
M. B. Scudiere
F. T. Sheldon

UT-BATTELLE
ORNL-27 (4-00)

ORNL/TM-2008/004

Computational Sciences and Engineering Division

ERROR REDUCTION FOR WEIGH-IN-MOTION

L. M. Hively
R. K. Abercrombie
M. B. Scudiere
F. T. Sheldon

Date Published: July 2008

Prepared by
OAK RIDGE NATIONAL LABORATORY
Oak Ridge, Tennessee 37831-6283
managed by
UT-BATTELLE, LLC
for the
U.S. DEPARTMENT OF ENERGY
under contract DE-AC05-00OR22725

CONTENTS

Page

Table of Contents

CONTENTS iii
LIST OF FIGURES v
LIST OF TABLES vii
ACKNOWLEDGMENTS ix
ABSTRACT 1
1. INTRODUCTION 1
2. CHARACTERIZATION OF ERROR IN WEIGHT 3
3. ANALYSIS METHODOLOGY 5
4. RESULTS FOR THE "TRAINING SET" 9
5. RESULTS FOR THE "TEST SET" 11
6. DISCUSSION 15
7. CONCLUSIONS 17
8. REFERENCES 19
Appendix A A-1
Appendix A. Tables and Figures A-3
Appendix B B-1
APPENDIX B: Mathematical Details of WIM Analysis B-3

LIST OF FIGURES

Figure **Page**

Figure 1. Weight measurement components and communication interfaces. A-17
Figure 2. Flow diagram for nonlinear analysis. A-18
Figure 3. Time-serial weight measurements versus time. A-19
Figure 4. Decrease in residual (filtered) WIM error versus mode number. A-20
Figure 5. Average percent error in the WIM vehicle weight versus vehicle speed. A-21
Figure 6. (WIM weight)/(IGS weight) versus IGS weight. A-22
Figure 7. Raw Weight Data for Hummer-BB06 Dataset. A-23
Figure 8. Sample standard deviation in the total WIM weight versus the time lag between the front- and rear-axle datasets for the Caravan-02 dataset without any clear minimum A-24
Figure 9. Sample standard deviation in the total WIM weight versus the time lag between the front- and rear-axle datasets for the F250-01 dataset with a clear minimum. A-25
Figure B-1. Labeling of *i*-th weigh pads B-3
Figure B-2. Locations of eight load cells in each WIM weigh pad. B-7

LIST OF TABLES

Table **Page**

Table 1. Time and motion study results A-3
Table 2. Percent error (16 vehicle configurations between 5,600 and 70,000 pounds) A-3
Table 3. Mode parameters for wrecker 6 analysis (item 12 of table 2) A-4
Table 4. Unfiltered error, e(u), and filtered error, e(n), in training sets A-5
Table 5. Characterization of test datasets A-5
Table 6. Mode-removal results for each wheel crossing of F-250 vehicle A-6
Table 7. Mode-removal results for each wheel crossing of freightliner truck A-7
Table 8. Mode-removal results for each wheel crossing of hummer H3 vehicle A-8
Table 9. Mode-removal results for each wheel crossing of silverado vehicle A-9
Table 10. Occurrence rate of error below 0.1% for single-wheel-crossing data A-10
Table 11. Occurrence rate of outliers for single-wheel-crossing data A-10
Table 12. Comparison of IGS and WIM from single-wheel crossings (pounds) A-10
Table 13. Mode-removal results for each axle of F-250 vehicle A-11
Table 14. Mode-removal results for each axle of freightliner truck A-12
Table 15. Mode-removal results for each axle of Hummer H3 vehicle A-13
Table 16. Mode-removal results for each axle of Silverado vehicle A-14
Table 17. Occurrence rate of error below 0.1% for single-axle data A-15
Table 18. Occurrence rate of outliers for single-axle data A-15
Table 19. Comparison of IGS and WIM for single-axle data (pounds) A-15
Table 20. Whole-vehicle, mode-removal results for F-250 vehicle A-16
Table B-1. Summary of WIM results B-11

ACKNOWLEDGMENTS

We gratefully acknowledge funding of this work by the ORNL Office of Technology Transfer's Technology (OTT) Maturation initiative. We specifically thank Casey Porto and Mark Reeves (OTT/ORNL) for their continuing encouragement and support of this work. We thank the following people for help with data acquisition: D.L Beshears, G.D. Richardson and C.P. White. We would also like to thank and acknowledge C.S. Case in the preparation of this manuscript.

ABSTRACT

Federal and State agencies need certifiable vehicle weights for various applications, such as highway inspections, border security, check points, and port entries. ORNL weigh-in-motion (WIM) technology was previously unable to provide certifiable weights, due to natural oscillations, such as vehicle bouncing and rocking. Recent ORNL work demonstrated a novel filter to remove these oscillations. This work shows further filtering improvements to enable certifiable weight measurements (error < 0.1%) for a higher traffic volume with less effort (elimination of redundant weighing).

1. INTRODUCTION

ORNL staff have developed and patented a portable system[1-22] (Fig. 1) that automatically obtains the following data from a vehicle that is driven slowly (≤5 MPH) over multiple weigh-pads on smooth asphalt or concrete surfaces: (1) weight on each tire; (2) single-axle weights; (3) total vehicle weight; (4) axle spacings; (5) longitudinal and transverse centers of balance; (6) wheel spacing on each axle; (7) vehicle length, width, and height; (8) an estimate of the vehicle volume from two-dimensional digital images; (9) vehicle identification via radio-frequency ID tag or barcode; and (10) cargo characterization. This system also provides: (11) a user-friendly interface (12) elimination of human error via automated data acquisition and analysis; (13) information infrastructure for secure, real-time, wireless transmission of results; (14) 60-80% reduction in personnel time versus in-ground scales (IGS) and wheel-weight scales, respectively; (15) 40% decrease in the number of personnel in comparison to wheel-weight scales; (16) greater operational flexibility; (17) improved safety; and (18) lower cost. The ORNL system is much more efficient than other existing methods, as summarized in Table 1. Alternative methods use static measurement of vehicle weight, a tape measure for determining axle distances, manual recording of individual axle weights and distances, manual calculation of total vehicle weight and center of balance, and manual entry of the results into a computer system.

The ORNL WIM efficiency advantages can be truly practical, when the error (Table 2) is comparable to (or less than) In-ground Scale (IGS) error for total weight. The measure of WIM performance is percent error in weight, which is defined as,

$$e = 100\left(\sigma / \overline{w}\right). \tag{1}$$

Here, $\overline{w}$ is the average vehicle weight, and σ is the sample standard deviation in the weight measurement; these quantities are explicitly defined in Section 3.

2. CHARACTERIZATION OF ERROR IN WEIGHT

Weight-measurement error arises from oscillations as a vehicle traverses the WIM system. These dynamics occur, because a vehicle is (i) a multi-body system of discrete masses (e.g., body, load, wheels) that are (ii) interconnected by springs (e.g., cab-load coupling, wheel suspensions) and are (iii) excited by various aperiodic forces (e.g., uneven terrain, steering changes, acceleration, wind variability, load shifts in liquids, engine vibration) with (iv) nonlinear damping by slip-stick friction and shock absorbers. Lower-frequency oscillations (1-5 Hz) arise from vehicle dynamics (e.g., side-to-side rocking, front-to-back rocking, vertical bouncing of the load on the suspension, load-bed flexure, twisting about coupling points, and nonlinear couplings among these modes). Higher-frequency oscillations (9-14 Hz) depend on vehicle size (e.g., tire rotation). Accurate weights require minimization of these oscillations, which WIM measurements presently reduce via a combination of: (a) minimal excitations by a smooth, flat, level approach, weighing, and exit; (b) constant, slow speed driving in a straight line; (c) several single-axle weight measurements as the vehicle crosses multiple weigh pads; and (d) continuous motion to foster dynamic friction, which reduces the slip-stick (static) friction. Further reduction of WIM error requires analysis of the time-serial weight data for removal of these vehicle oscillations.

A model for the vehicle oscillations, $x(t)$, over time, t, uses a second-order, ordinary differential equation:

$$m\frac{d^2x}{dt^2}+\gamma\frac{dx}{dt}+kx=F(t). \tag{2}$$

The variable m is the vehicle mass; γ is the damping coefficient; k is the spring constant for the vehicle suspension; and the forcing function is:

$$F(t)=A\cos(\omega t). \tag{3}$$

The solution[23] is:

$$x(t)=(A/G)\sin(\omega t-\delta), \text{ where } \delta=A\cos(\gamma\omega/G). \tag{4}$$

The resonance term is:

$$G=\sqrt{m^2(\omega^2-\Omega^2)+\gamma^2\omega^2} \text{ with } \Omega=\sqrt{(k/m)}. \tag{5}$$

Real-world forces usually have multi-modal forcing functions of the form,

$$F=\sum_j F_j\cos(\omega_j t+\phi_j). \tag{6}$$

Each mode has a different amplitude (F_j), frequency (ω_j), and phase (ϕ_j). Here, Σ_j indicates summation over the various forcing modes. The net response to such multi-modal driving functions is the sum of the periodic solutions with a relative phase shift:

$$x(t)=\sum_j(A_j/G_j)\sin(\omega_j t-\delta_j+\phi_j). \tag{7}$$

If the forcing-function parameter values are available, then this approach can determine the mass from the vehicle oscillations. However, the forcing-function parameters are <u>not</u> known, and <u>cannot</u> be inferred

from the time-serial weight data. Also, the arbitrary phase (ϕ_j) obscures the deterministic phase (δ_j) that can be used with the resonance factor (G) to determine the mass.

3. ANALYSIS METHODOLOGY

The considerations of the previous section lead to the conclusion that the vehicle oscillations must be removed empirically to reduce the WIM measurement error. Consequently, this work decomposes the time-serial WIM weight measurement, $W(t)$, into the form:

$$W(t) = w + \sum_j A_j \sin(\omega_j t + \varphi_j)\, e^{\alpha_j t}. \tag{8}$$

Here, w is the filtered vehicle weight that WIM seeks to measure. The j-th sinusoidal mode is characterized by an amplitude (A_j), frequency (ω_j), and phase (φ_j). The summation, Σ_j, is over all of the oscillatory modes. The test data have both exponential growth ($\alpha_j > 0$) and decay ($\alpha_j < 0$) of sinusoidal modes, which are modeled by the term, $e^{\alpha_j t}$. Re-arrangement of Eq. (8) extracts the filtered weight:

$$w(t) = W(t) - \sum_j A_j \sin(\omega_j t + \varphi_j)\, e^{\alpha_j t}. \tag{9}$$

The left-hand side of Eq. (9) shows explicit time dependence in the filtered weight, $w(t)$, because the right-hand side is time dependent. Indeed, the results of Sect. 4 show that the filtered weight has residual time-variability, even after removal of many oscillatory modes. Experimental data from recent WIM tests were obtained at a sampling rate of 1,000 Hz ($\Delta t = 0.001$ second) as vehicles traversed the two-foot-long weigh pads. Minimal transients in the weight data occur in the central (one foot) section of the weigh pad, corresponding to a "flat-top" interval that was used for the weight-determination analysis. The flat-top region was traversed in < 200 milliseconds, allowing acquisition of many cycles of the fast dynamics, and less than one cycle of the slow oscillations. Consequently, the values of $W(t)$ are available only at discrete time values, which are denoted by $W(t) = W(i\Delta t) \equiv W_i$. The corresponding discrete form for the filtered weight values are denoted by $w(t) = w(i\Delta t) \equiv w_i$. The discretized form of Eq. (9) then becomes:

$$w_i = W_i - \sum_j A_j \sin(i\omega_j + \varphi_j)\, e^{i\beta_j}, \text{ with } \beta_j = \alpha_j \Delta t. \tag{10}$$

Equations (8) – (10) are a generalized finite-Fourier decomposition[24] of the vehicle oscillations for discrete frequencies, $\omega_j = j\pi/2N$, where the symbol, N, denotes the number of data points in the flat-top region. Very short flat-top intervals ($N < 10$) are ignored in this analysis. The average vehicle weight, $\overline{w}$, then is:

$$\overline{w} = (1/N)\sum_i w_i. \tag{11}$$

The corresponding sample standard deviation, σ, in the vehicle weight is given by:

$$\sigma = \sqrt{\sum_i (w_i - \overline{w})^2 / (N-1)}. \tag{12}$$

The summations in Eqs. (11) – (12) are from i=1 to N. The resultant percent error, e, in the vehicle weight is:

$$e = 100(\sigma/\overline{w}). \tag{13}$$

Eqs. (11) – (13) apply with or without the removal of any oscillation modes in Eq. (10). With these derivations, the specific analysis methodology (via MatLab[25]) can be described.

After initializations, the analysis code reads the stream of time-serial WIM data, and extracts the flat-top region of N data points. This step is labeled (A) in Fig. 2. All subsequent steps are labeled sequentially in Fig. 2, and involve analysis of this same flat-top region of N data points. Step (B) obtains the unfiltered WIM weight error via Eqs. (11) – (13) without any mode removal; that is with $w_i = W_i$. Subsequent steps, beginning with the loop initialization in step (C), remove each successive oscillatory mode.

Step (D) performs a standard finite-Fourier transform[18] (*fft* function in MatLab) of the time serial data to estimate the mode parameters, using the following forms:

$$A_j = \sqrt{B_j^2 + C_j^2}\ , \tag{14}$$

$$\varphi_j = \arctan\left(B_j / C_j\right). \tag{15}$$

Here, the symbols, B_j and C_j, denote the amplitude of the unshifted cosine and sine terms, respectively:

$$W(t) = B_0/2 + \sum\nolimits_j B_j \cos\left(2\,j\pi\,t/N\right) + C_j \sin\left(2\,j\pi\,t/N\right), \tag{16}$$

$$\omega_j = 2\,j\pi/N\ . \tag{17}$$

The specific value for the mode frequency is the smallest value with:

$$A_j \geq 0.9 \max \sqrt{B_j^2 + C_j^2}\ . \tag{18}$$

Here, the maximum (*max*) is taken from all of the FFT amplitudes from Eq. (14), corresponding to the largest mode amplitude from the FFT. If the largest possible amplitude is always used to choose the mode frequency, then very high order frequencies can be chosen, when in fact a low-frequency mode also has a large, but non-maximal amplitude, and thus is more appropriate for removal. The above choice resolves this spurious removal of high-order modes.

Step (E) uses the mode-parameter estimates from step (D), together with a very crude guess for the mode growth (α_j =0.0001), as the starting point for a 4-parameter search over the set, $\{A_j, \omega_j, \varphi_j, \alpha_j\}$, to minimize the error for removal of the j-th (single) mode. The specific MatLab function is *fminsearch*. If the value of optimal frequency is within 10% of the estimate from step (C), then the parameter values are acceptable, and are used as for the next step (F). If the optimal frequency is outside this 10% limit, then the search is repeated with the original estimates of A_j and ω_j, from Eqs. (14) and (17), respectively, but with a random starting point for the phase, $\varphi_j = 2\pi\rho$, and for the growth rate, $\alpha_j = 0.001(2\rho - 1)$. Here, the symbol, ρ, denotes a uniformly-chosen random number between zero and one, via the MatLab function, *rand*. If twenty iterations of this random re-initialization do not find an optimal frequency within 10% of the original estimate, then the smallest-error parameter set is used for the next step.

Step (F) converts the frequency value from the previous optimization search to the nearest integer multiple of the "fundamental" frequency, $\omega_f = \pi/2N$. The value of ω_f is half of the value for a standard FFT, because (as explained above), the short-time sampling of the WIM weight data can only acquire less than one cycle of the slow oscillations. Other values of ω_f were tested, but gave poorer filtering results. If

ω_j is allowed to have any (continuous) value, then two successive modes can have very close values of frequency that beat against each other, yielding non-physical results.

Step (G) uses the fixed, discrete value of $\omega_j \leq 2\pi$ from step (F) and the other optimal parameters from step (E) as the starting point for a second search. This search also uses the MatLab function, *fminsearch*, to minimize the error over the 3-parameter search space, $\{A_j, \varphi_j, \alpha_j\}$. Sometimes, the search results have unphysical values (e.g., $A_j < 0$ or with an excessive magnitude, or with $\omega_j < 0$), which requires conversion of the parameter values to a "regular" form, in step (H). In some instances, the frequency value can validly have the value, $\omega_j = \pi$; that is, $k = N$. In this case, the j-th term in Eq. (10) involves the term:

$$A_j \sin\left(i\omega_j + \varphi_j\right) = A_j \sin\left(i\pi + \varphi_j\right) = A_j \cos(i\pi)\sin\left(\varphi_j\right) = A_j(-1)^i \sin\left(\varphi_j\right). \tag{19}$$

The analysis converts both A_j and φ_j, as follows:

$$A_j \leftarrow A_j \sin\left(\varphi_j\right);\ \varphi_j = sign\left[(-1)^i\right]. \tag{20}$$

The replacement of A_j with $A_j\ sin(\varphi_j)$ avoids a large magnitude that usually occurs for A_j in this case with φ_j typically close to π. Three further sequential steps complete conversion to a regular form:

$$A_j \leftarrow -A_j, \text{ and } \varphi_j \leftarrow \varphi_j + \pi, \text{ if } A_j < 0, \tag{21a}$$

$$\varphi_j \leftarrow \varphi_j + 2\pi, \text{ if } \varphi_j < 0, \tag{21b}$$

$$\varphi_j \leftarrow \mathrm{mod}_{2\pi}\left(\varphi_j\right), \text{ if } \varphi_j > 2\pi. \tag{21c}$$

Eq. (21a) assures $A_j > 0$. Eq. (21b) assures $\varphi_j > 0$. Eq. (21c) assures $0 \leq \varphi_j \leq 2\pi$, by subtracting integer multiples of 2π from φ_j until the appropriate range is achieved. Eqs. (21a) – (21c) are also imbedded in step (E). If the resultant error is not lower than that for removal of the previous mode, then the search is repeated (up to 20 times) with the original fixed, discrete value of ω_j from step (F) and with random starting points for the amplitude, $A_j = 2\rho\ A_j(\mathrm{E})$, and for the phase, $\varphi_j = 2\pi\rho$, and for the growth/decay rate, $\alpha_j = 0.001(2\rho - 1)$. Here, $A_j(\mathrm{E})$ is the optimal amplitude from step E.

Step (I) saves the parameter values, the resultant error, and the residual weight values, w_i, after removal of the j-th oscillatory mode. Step (J) repeats Steps (C) - (I) to remove an additional mode with W_i now equal to the residue after removal of the present mode. Step (J) terminates the mode-removal loop, if the resultant error is not smaller than that after removal of the previous mode. Step (J) also terminates the mode-removal loop, when the number of modes removed, M, reaches *floor*(N/3). The MatLab function, *floor*, rounds a positive number down to the next smaller integer. This limit avoids over-fitting of the total number of modes that are filtered, because N is the maximum number of degrees of freedom for mode removal (with the frequency values fixed at discrete values). The degrees of freedom are allocated among the 3 parameters, $\{A_j, \varphi_j, \alpha_j\}$, for each of the M modes, implying $3M \leq N$, yielding the above limit. Step (K) saves the results of the mode-filtering analysis, including the error for each mode removal step, the resultant parameter values, and the residual weight over time. Step (L) returns the analysis to step (A), if additional WIM data are available. Otherwise, the analysis is stopped. This algorithm is very robust, namely one that analyzes all of the datasets (Sect. 4) without user intervention.

We also comment about the repeated used of the local-search MatLab routine, *fminsearch*, rather than a global optimizer. First, the use of *fminsearch* yields excellent results, as discussed below. Second, a

simultaneous search over all of the modes is extremely slow, and does not improve the filtered error. Consequently, we omitted a global search in favor of one-at-a-time removal of each oscillatory mode.

4. RESULTS FOR THE "TRAINING SET"

The present WIM data acquisition hardware (MC12S series 8/16-bit micro-processor) was adapted to acquire time-serial data from the last wheel crossing of the last WIM weigh pad. This effort included software updates to the host computer for the data acquisition for up to ten independent, time-serial weight measurements from each of several vehicles. These data were the "training" set for development of a methodology (Sect. 3) to reduce weight variability from vehicle dynamics.

Twenty-eight (28) time-serial datasets were obtained during WIM field tests at Fort Lewis (Pierce County in the State of Washington) on October 3-6, 2006. Two military vehicles were each weighed six times: a Stryker armored vehicle (total weight < 12 tons) and a military wrecker (total weight > 12 tons). A civilian station-wagon-class vehicle (Suburban) was also weighed ten times without a load, and again six times with a 200-pound load. All four sets of data were analyzed as part of the methodological "training" set to provide a robust filtering algorithm to reduce the WIM measurement error.

Figure 3 shows a typical result of this analysis. Figure 3a displays the unfiltered time-serial weight data (solid line) for a military wrecker vehicle (item 12 in Table 3). The left side of Fig. 3a shows the unfiltered error (ERROR=0.97438%), the mean weight (MEAN=6400.879), and the number of points in the flat-top segment (N=157). The raw data in this example fall erratically from a maximum to a similarly erratic minimum. The underlying trend is roughly one-half of a sine wave, which is removed via the empirical-fitting methodology of Sect. 3. The resultant best-fit curve for this first mode is shown by the dashed curve in Fig. 3a, and is typical of the time-serial dynamics for heavy vehicles. Figure 3b illustrates the residual variability (solid line) after removal of the partial sine-wave of Figure 3a; the corresponding mean and percent error of the residue are at the right of the subplot, as before. The residual time-serial weight data have an erratic 2-period sine wave with a corresponding best-fit (dashed-line) curve, the removal of which leaves the residue in Fig. 3c with a further error reduction. Figures 3c-3d display the residue and percent error after removal of two more oscillatory modes. Figure 3e shows the residual error versus time after removal of 52 modes. Table 3 shows representative parameters for the removal of each mode: amplitude (A_j), frequency (ω_j/ω_f), phase (φ_j), growth/decay rate (α_j), and residual error (e). The residual error for removal of 52 modes is 0.045%, which is well below the 0.1% limit.

Table 4 summarizes the percent-error results from filtering analysis for all of the training vehicles. Table 4 shows multiple entries under the same dataset name, corresponding to several, distinct wheel crossings in the same dataset. The large unfiltered errors in the SuburbanF series of Table 3 are noteworthy, and arise from the small number of data points in the flat-top region. The average transit time was 41ms to cross the central one-foot region of the weigh pad. The corresponding transit speed was 16.6 MPH, which is more than three times faster than the recommendation of ≤5 MPH, for which the low-error results were obtained for the Stryker and Wrecker series. Table 4 also shows the average error without and with mode filtering. The column, e(u), presents the unfiltered error. The columns, $e(1) - e(3)$, show the error after removal of one, two, and three sinusoidal modes, respectively. The column, $e(M)$, shows the filtered error after removal of M modes. The bold-face entries are the average errors for each series. For example, Stryker series has average errors of 1.355%, 0.227%, 0.214%, 0.201%, and 0.047% for removal of zero, one, two, three, and M modes, respectively. These results clearly show that high-order mode-filtering reduces the WIM error below the 0.1% level for slow-speed vehicle-weight measurements.

Figure 4 shows the percent error, $e(k)$, versus the number of filtered modes, $k \le M$. Figure 4a shows $e(k)$ versus k for each of the Stryker-series measurements, reaching $e(k) < 0.1\%$ for $24 \le k \le 44$. Figure 4b shows $e(k)$ versus k for each of the Wrecker-series measurements, reaching $e(k) < 0.1\%$ for $17 \le k \le 37$. Figure 4c shows $e(k)$ versus k for each of the Suburban-series of measurements, for which smallest error is 0.161% (item 20 of Table 4) after removal of 47 modes. Figure 4d shows $e(k)$ versus k for each of the

SuburbanF-series of measurements, for which smallest error is 0.21% (item 20 of Table 4) after removal of 13 modes. These plots clearly show the consistency in mode-removal for low-error results from slow vehicles, and the greater spread (inconsistency) in mode-removal from higher-speed vehicles.

Figure 5 summarizes the results from Fig. 4 into a single plot of error versus vehicle speed. The left-most column of points (*) corresponds to the average of the Stryker-series of measurements at an average speed of 4 MPH. The second column of points from the left is the Wrecker-series of measurements at an average speed of 4.3 MPH. The second column of points from the right is the Suburban-series of measurements at 5.6 MPH. The right-most column of points shows the SuburbanF-series of measurements at an average speed of 16.6 MPH. The top curve (solid blue) is the unfiltered error for each of the vehicles with errors ranging from 0.857% (Wrecker) to 3.397% (SuburbanF). The second curve from the top (dashed red) shows the filtered error after removal of one mode with errors ranging from 0.294% (Stryker) to 2.113% (SuburbanF). The third curve from the top (chain-dashed purple) shows the filtered error after removal of two modes with errors ranging from 0.216% (Wrecker) to 1.747% (SuburbanF). The second curve from the bottom (solid green) displays the filtered error after removal of three modes with errors ranging from 0.199% (Wrecker) to 1.448% (SuburbanF). The bottom curve (dashed magenta) illustrates the filtered error after removal of all M modes with error ranging from 0.048% (Wrecker) to 0.374% (SururbanF). The floor in the filtered error at ~4 MPH suggests that this speed (but probably not less) will minimize the error in WIM weight measurements. Figure 5 also shows that removal of many oscillatory modes significantly reduces the error at all speeds.

5. RESULTS FOR THE "TEST SET"

A second set of WIM time-serial measurements was acquired for a realistic demonstration of the mode-filtering, error reduction approach. Adequate statistics require ten (or more) independent measurements from each of several vehicles. This effort involved the following work on two WIM weigh pads: (a) addition of a 16-channel National Instruments™ data acquisition system; (b) testing and debugging of the hardware from (a); (c) software to acquire the 8-channel data from each weigh pad for each wheel crossing from (b); (d) software to convert the independent data channels from (c) into total-pad weight for each wheel crossing at each sampling time; (e) software to extract the flat-top region from (d); (f) software to provide the time-serial, total-pad weight data from both sides of the vehicle for (g) subsequent analysis by the mode-filtering algorithm from Section 3. The experimental test protocol was as follows.

1) Weigh the vehicle on a certified IGS;
2) Weigh the vehicle via the ORNL WIM system, as modified above;
3) Repeat step 2 many times for each vehicle;
4) Weigh the vehicle on a certified IGS;
5) Repeat steps 1-4 for each of several vehicles.

Steps 1 and 4 provide two identical and independent weight measurements from the IGS for each vehicle. Steps 2 and 3 provide several identical and independent weigh-in-motion measurements for the same vehicle. This protocol allows a statistical comparison of the mode-filtered WIM weights (with a corresponding standard deviation) to the IGS measurement, which is certified to a standard deviation of < 0.1% for total weight only. This protocol also allows calibration of the mode-filtered WIM weight to the certified IGS measurements. On the basis of the results in Sect. 4, all vehicles were driven slowly across the WIM weigh pad, resulting in many more data points for each wheel crossing of a pad.

Test data were obtained at ORNL's National Transportation Research Center on May 8-10, 2007. Four vehicles were weighed: Ford F-250, Freightliner truck, General Motors H3 Hummer, and Chevrolet Silverado. Weight data were obtained from two pads that simultaneously measured the left- and right-side tires as the vehicle was driven over the WIM system. Three datasets (all from the Hummer) had time-serial weight data for only one axle (two wheel crossings); the rest (125 datasets) included data from two axles (four wheel crossings for the F-250 and Silverado) or three axles (six wheel crossings for the Freightliner truck). Each vehicle was weighed in three different ways: (1) driving the vehicle normally across the weigh pads; (2) adding a ½" bump before crossing the weigh pads; and (3) adding a 1" bump before the weigh pads. The weight for a single weigh-pad crossing varied from 900 pounds for the Silverado to 5,500 pounds for the Freightliner truck. Table 5 characterizes the data for each vehicle, showing that the IGS variability is up to 10/4645, or 0.215% (more than twice the certified error). A data quality check revealed that most of the datasets have one (or more) weight value(s) at the end of each weigh-pad crossing that are inconsistent with the other data (e.g., dramatically higher or lower than the other values). These transient points were removed before application of the mode filtering algorithm.

Tables 6-9 summarize the results in terms of the mode-filtered minimum error, e(min), in percent, and the corresponding average weight, $\overline{w}$, in pounds for each wheel crossing. These results are shown for the F-250 (Table 6), the Freightliner truck (Table 7), the Hummer-H3 (Table 8), and the Silverado (Table 9). Mode-filtered error values above 0.1% are shown in **bold** font. Some values of $\overline{w}$ are outliers, namely different from the non-outlier, column-average, $\overline{\boldsymbol{w}}$, by more than two standard deviations. The value of $\overline{\boldsymbol{w}}$ and the corresponding standard deviation, $\boldsymbol{\sigma}$, are initially determined by a column-average over all $\overline{w}$ -values. Any $\overline{w}$ -value was excluded if $|\overline{w} - \overline{\boldsymbol{w}}|/\boldsymbol{\sigma} > 2$. The non-outlier $\underline{w}$-values were next used to obtain a new estimate of $\overline{\boldsymbol{w}}$ and $\boldsymbol{\sigma}$, which were used to remove additional outlier $\overline{w}$ -values by the same criterion. This process is repeated until no new outliers were identified. An underline denotes these $\overline{w}$ -outliers, which occur in many cases even though the mode-filtered error is below 0.1%. The total vehicle weight, $\overline{W}$, (right-most column) in each table is the row-sum over the all wheel-weight values. The

outlier-rejection algorithm also was applied to the total weight values. We note that the *e*(min) value quantifies the *precision* of $\overline{w}$, while the value of $|\overline{w} - \overline{\boldsymbol{w}}|/\boldsymbol{\sigma}$ quantifies the *accuracy* of $\overline{w}$. All weights are rounded to the nearest pound, because more precision is unjustified by the corresponding errors values, which are ≥10 pounds. Clearly, an important subject for future work is a method to reject outlier measurements.

The two weigh pads for acquisition of this data were part of a larger 8-pad WIM system. The 6-pad WIM sub-system that did not include the two pads for recording this data flagged no problems with the data acquisition. However, the 6-pad WIM sub-system that included the two pads for recording the present data flagged many problems. One problem involved ambiguous (noisy) raw data, as denoted by an 'X' in the second column of Tables 6-9. Another problem was an excessively large value of BadSpdRms, as denoted by 'S' in the second column of Tables 6-9. (See Appendix A for a detailed description of the multiple-pad WIM system, and the methodology for inferring the WIM measurements and problems.) No clear correlation exists between these flags, and the bold or underlined weight values in Tables 6-9. These problems might have arisen from noise on the additional (unshielded) wires for acquisition of the present (analog) data. Noise might have originated from concurrent experiments in nearby test cells. One solution is more careful grounding and shielding of the WIM data acquisition system in future experiments.

Further study of Tables 6-9 reveals that two columns of wheel crossings have all *e*(min) values below 0.1% (i.e., the first wheel crossing in Table 7 and the fourth wheel crossing in Table 9), while other wheel crossings from the same vehicle have many *e*(min) values above 0.1% (e.g., second, third, and sixth wheel crossings in Table 7). This result suggests that pad-level differences can influence the mode filtering. This problem needs further study, involving pad calibration, precision, and related issues.

Table 12 summaries the test results in terms of the number of error values (precision) below 0.1% from Tables 6-9. We note several important features in Table 10. First, the best results for the no-bump case are for the F-250 (61/64 = 95%) and FreightLiner (86/102 = 84%), which is the only heavy commercial-class vehicle (> 15,000 pounds) in these experiments. Second, the best results for the ½"-bump case are for the Hummer (26/28 = 93%) and the Silverado (24/24 = 100%). The 1"-bump results show higher errors in all cases. The total rate of sub-0.1% error is 197/218 or 90%. Third, the counter-intuitive decrease in error with a small bump (½") arises from excitation a larger, more-easily-removed oscillation, which overwhelms (and thus excludes) other less-easily-removed periodicities. However, Table 11 shows that the number of outliers (a measure of accuracy) is much lower for the non-bump cases. Consequently, the "bump" approach improves the precision (Table 10), but worsens the accuracy (Table 9) for the single-wheel-crossing data. More precise but less accurate single-wheel weights are not helpful.

Table 10 compares the WIM and IGS weights for each vehicle. The single-axle WIM weights were obtained by summing the appropriate values in Tables 6-9, rejecting the outliers, and then calculating the resultant average and standard deviation (value in parentheses) as before. The two weight values in each IGS column correspond to the pair of measurements from the above protocol. Figure 6 shows the results from Table 12 for total weights (subplot a), single axle weights (subplot b), and a combination of the total and single-axle weights (subplot c). The WIM weight is normalized by the corresponding IGS weight in each case, namely Y = (WIM weight)/(IGS weight), with error bars of one standard deviation. A least-square, straight line provides an excellent fit to these data in all cases with the fitting parameters shown in each subplot. Figure 6c shows that the WIM weight measurements are systematically low by 2.6%, and rise slightly (0.03% per 1,000 pounds) with increasing weight. We emphasize that only the total IGS weight is certified to an error of < 0.1%, which is consistent with the WIM weight results. These results show that mode-filtering achieves a measurement error of < 0.1% in 90% of the best cases.

Some mode-filtered errors in Tables 6-9 are large; Table 8 shows the biggest errors (0.38-0.46%) for the Hummer-BB06 dataset. Figure 7 shows the time-serial data for this case with large spikes (a rise or fall

over a single time step). Quality analysis[26] of the unfiltered data can reject such data from further analysis. However, careful study reveals that many datasets have such spikes, which are usually associated with a weight offset (also illustrated in Fig. 7), meaning that the typical weight value before the spike is different than afterward. Other datasets have large "bumps" (a rise or falls over several time steps), which are usually the first (large) oscillations in a decaying sequence. Some bumps are also associated with weight offsets, which clearly correspond to the suspension sticking in a new position after oscillation damping. Apparently, the spikes with an associated weight offset are the same phenomena in a stiff (highly damped and rapidly oscillating) suspension. We further note that the offsets for the two wheel crossings have opposite signs, corresponding to side-to-side rocking.

A novel solution to the spike-bump problem is to sum the two single-wheel datasets for each axle into a single-axle dataset, and then to mode-filter the sum as before. This approach has several advantages: (a) determination of single-axle weight (which is adequate for highway inspection stations); (b) implicit removal of side-to-side rocking; (c) reduction of the number of mode-filtered datasets by half; (d) lower mode-filtered error, as discussed below; and (e) faster computational analysis. Tables 13-16 show the results of this single-axle mode-filtering analysis. Table 13 shows that only one instance of error above 0.1% occurs for the F-250, that the values of $e(min)$ are smaller than the single-wheel-crossing values, and that $\sigma/\overline{w}$ is slightly lower for total weight than in Table 6. We note that the large- and small-bump results deviate systematically from the F-250 average, although most of those weights are within two standard deviations of the average. If only the non-bump data are used for the mean and standard deviation with exclusion of outliers, then two values are excluded (#03 and 17), as denoted by the *italic* weights in Table 13. Then, the non-bump F-250 total-weight average (7196 pounds) and standard deviation (39 pounds) yield $\sigma/\overline{w} = 0.55\%$, which is a substantial improvement over 1.9% in Table 6, and 1.8% in Table 13. Similar single-axle improvements occur for the FreightLiner truck (Table 14), the Hummer H3 (Table 15), and the Silverado (Table 16). Table 17 shows that the single-axle error (precision) is uniformly lowest for the ½"-bump case. Table 18 shows that the corresponding number of outliers (a measure of accuracy) is consistently smallest for the non-bump case. More precise but less accurate single-axle weights are not helpful, so we must reject the use of ½"-bump cases as less accurate. Table 19 shows the corresponding comparison of IGS and mode-filtered-WIM single-axle weights, which are not unlike the plots in Fig. 6, and hence are not shown.

A third set of WIM time-serial measurements were acquired on September 17, 2007 at ORNL's National Transportation Research Center. This experiment involved the same test protocol as the previous "test" set with in-ground scale measurements after every 3 to 7 WIM crossings (eight IGS measurements). This experiment used two 16-channel National Instruments™ data acquisition systems to acquire time-serial weights simultaneously from both the front and back axles of three vehicles (Ford F-250, Hummer H3, and Caravan) at a sampling rate of 4 kHz. On the basis of the improvements via single-axle weights, the front and back axle weight data are summed to obtain total-vehicle weight versus time, thus implicitly removing side-to-side rocking, front-to-back rocking, and vertical bouncing prior to the application of the mode filtering algorithm. However, the use of a 16-channel data acquisition system for each axle did not allow sufficiently accurate synchronization of the weight data from each axle to obtain total weight directly. Consequently, the time lag between the front and rear weight data was varied to find the minimum sample standard deviation in the total weight. Figure 7 shows an example of this deviation-versus-lag plot for the Caravan-02 dataset. This plot displays no clear minimum due to a lack of time-serial synchronization in WIM data, since WinXP is not a real-time operating system in starting the two data acquisition systems. All Caravan and Hummer-H3 datasets displayed this same non-synchronization. Figure 8 shows a second example of the deviation-versus-lag for the F250-01 dataset, displaying strong maxima on either side of the clear minimum (denoted by the red star in the top plot). We focus the subsequent analysis on the twenty F-250 datasets that had such a clear minimum. Figure 8 (bottom plot) shows the resultant (unfiltered) time-serial total-weight data after summing the front- and back-axle weight data with the lag from the top subplot. Table 20 summarizes the results after application of the

mode-filtering algorithm to these total-weight data, including the unfiltered error, $e(u)$ (second column), the filtered error, $e(min)$ (third column), and total weight, $\underline{W}$ (right column). These results are a substantial improvement over the previous results, namely: (1) all error values, $e(min)$, are well below 0.1% after mode removal; (2) all of the filtered-weights occur within two standard deviations of the average (no outliers); (3) total weight is consistent with the certification requirement, in contrast to single-wheel or single-axle weights as analyzed above. Consequently, the use of mode-filtering on the total weight data provides both lower error (more precise), as well as more accurate (no outlier) values.

6. DISCUSSION

Error reduction below 0.1% via mode filtering results in essentially no further change in the WIM weight. Consequently, a substantial speed improvement in the mode-filtering algorithm is possible by termination of the analysis, when the error reaches this limit. The residual weight variability after completion of the mode filtering has a complex waveform (e.g., Figure 3e) that is reminiscent of nonlinear time-serial data from other analyses[27]. The use of an explicitly nonlinear, statistical approach for WIM error reduction may therefore be useful. These ideas provide avenues for further development effort.

The achievement of sub-0.1%-error in the WIM system enables further technology development, on which we comment next. First, this error level corresponds to < 6 pounds in a 6,000-pound wheel weight for heavy vehicles. The weigh-pad calibration error is presently ±50 pounds for ≤ 5,000 pounds and ±100 pounds for 5,000 – 17,000 pounds. Consequently, improvement in WIM accuracy will require better calibration, and/or more accurate sensors (presently stain-gauge based). Second, further reduction in WIM error also requires improvement in the present 12-bit analog-to-digital (A-to-D) conversion, which corresponds to one part in 2^{12} = 4,096 or ~1.5 pounds in a 6,000-pound wheel weight. Commercial data acquisition systems can now provide 16-bit A-to-D conversion or $6000/2^{16}$ ~ 0.1 pound, which is more than adequate. Third, this same error level is desirable at higher vehicle speeds, for which a longer weigh-pad length is appropriate. Specifically, a vehicle tire crosses the central one-foot of the present WIM weigh pad in 170 milliseconds at 4 MPH, corresponding to acquisition of 170 data points in the flat-top region at a sampling rate of 1,000 Hz. The larger error for the Suburban vehicle (Table 1) occurred, because the higher vehicle speed (> 15 MPH) restricted the data acquisition to far fewer data points for the error reduction analysis. Consequently, a longer weigh-pad length (e.g., 3 feet long, depending on a cost-benefit analysis) would provide a 2-foot central region for adequate data at 10 MPH. (We also note that the Suburban-vehicle weight results are not typical of heavy commercial vehicles, for which the WIM system is intended.) All of these further improvements involve straight-forward development paths, and would substantially enhance the commercial use of the WIM measurement system in collaboration with an industrial partner. These ideas for development will substantially enhance the WIM technology.

7. CONCLUSIONS

Over the last decade, ORNL staff have developed and patented a substantial portfolio of intellectual property (IP) for the WIM technology[1-8]. The present work provides an additional and significant improvement to the WIM technology and the corresponding intellectual property[9]. Namely, this work demonstrates a mode filter that reduces the error in WIM weight measurements to < 0.1%. This error is comparable to that from certified IGS scales. Thus, the ORNL WIM technology has the efficiency and safety advantages of a weigh-in-motion system, together with an error level comparable to IGS. This report formally documents the WIM error-reduction work, including intellectual property improvements.

The second specific benefit of this reduction of WIM weight-measurement error is increased interest in commercialization of this ORNL IP. We have identified two interested parties, with whom we have discussed licensing of the technology. ORNL staff will continue to work with ORNL's Office of Technology Transfer (OTT) to interest such potential partners in the technology.

The third benefit of this advancement is a commercializable prototype with both lower measurement error and greater efficiency than competing technologies, as discussed in the Introduction. Certification of the WIM technology for < 0.1% error requires many additional measurements (many hundreds to thousands) to provide a solid statistical basis. The present work provides a clear path to certification.

8. REFERENCES

[1] J. D. Muhs, M. B. Scudiere, and J. K. Jordan, "Method and apparatus for converting static in-ground vehicle scales into weigh-in-motion systems," *US Patent #6,459,050* (October 1, 2002).

[2] D. L. Beshears, G. J. Capps, J. K. Jordan, J. V. LaForge, J. D. Muhs, R. N. Nodine, M. B. Scudiere, and C. P. White, "System and methods for accurately weighing and characterizing moving vehicles," *US Patent #5,998,741* (December 7, 1999).

[3] D. L. Beshears, G. J. Capps, J. K. Jordan, J. V. LaForge, J. D. Muhs, R. N. Nodine, M. B. Scudiere, and C. P. White, "System and method for accurately weighing and characterizing moving vehicles," *US Patent #5,959,259* (September 28, 1999).

[4] J. D. Muhs, J. K. Jordan, K. W. Tobin, and J. V. LaForge, "Apparatus for weighing and identifying characteristics of a moving vehicle," *US Patent #5,260,520* (November 9, 1993).

[5] D. L. Beshears, S. G. Batsell, R. K. Abercrombie, M. B. Scudiere, and C. P. White, "System and method for identifying, validating, weighing and characterizing moving or stationary vehicles and cargo," *US Patent #7,305,324 B2* (December 4, 2007).

[6] D. L. Beshears, M. B. Scudiere, and C. P. White, "System and method for weighing and characterizing moving or stationary vehicles and cargo," *Divisional US Patent Application #11/550,482* (October 18, 2006).

[7] R. K. Abercrombie and B. G. Schlicher, "Method and System for Determining a Volume of an Object from Two-Dimensional Images," *US Patent Application #11/583,473* (October 18, 2006).

[8] "Geo-registration of Images/Videoframes Using Mulitple Data Sources Including Telemetry, Geo-registered Elevation and Image Data, Pattern and Feature Recognition," Patent IDEA 05-127.

[9] L. M. Hively and R. K. Abercrombie, "Reducing Errors in Vehicle Weighing Systems," *Provisional US Patent Application #61/003,095* (November 14, 2007).

[10] R. M. Walker, R. K. Abercrombie, and S. G. Batsell, "Performance Based Commercial Vehicle Inspection System," *US Patent Application #11/703,992* (February 8, 2007).

[11] K. W. Tobin, and J. D. Muhs, "Algorithm for a novel fiber-optic weigh-in-motion sensor system," *ORNL/TM-2003/538* (Oak Ridge National Laboratory, Oak Ridge, TN) 2003.

[12] R. K. Abercrombie, J. E. Coats, Jr., and R. B. Honea, "Weigh-In-Motion (WIM) Technology for In-Theater Applications," *83rd Annual Meeting of Transportation Research Board,* Washington, DC USA, January 14, 2004.

[13] J. E. Coats, Jr., R. K. Abercrombie, D. L. Beshears, and R. B. Honea, "Weigh-In-Motion Technology for Military Operations: Developing a Portable, Safe, and Accurate System," *TR News - Transportation Research Board of the National Academies*, vol.231, March-April 2004 pp.16-18.

[14] R. K. Abercrombie, F. T. Sheldon, B. G. Schlicher, and K. M. Daley, "Development of the Joint Weigh-In-Motion and Measurement Reach Back Capability - The Configuration and Data Management Tool for Validation, Verification, Testing and Certification Activities," *Logistics Spectrum*, Volume 38, Issue 4, 2004, p. *4-9*, (published December 2005).

[15] R. K. Abercrombie, "Weigh-in-Motion (WIM) Research and Development Activities at ORNL," *4th International Conference on Weigh-in-Motion*, Taipei, Taiwan, February 21, 2005.

[16] R. K. Abercrombie, D. L. Beshears, M. B. Scudiere, J. E. Coats, Jr., F. T. Sheldon, C. Brumbaugh, E. Hart, and R. McKay, "Weigh-In-Motion Research and Development Activities at the Oak Ridge National Laboratory," *Proceeding of 4h International Conference on Weigh In Motion*, Taipei, Taiwan, National Science Council, National Taiwan University Publications (ISBN 986-00-0417-X), 2005 pp.139-149.

[17] R. K. Abercrombie, "Next Generation Weigh-In-Motion: Enhancing Weighing and Measuring of Military Vehicles/Cargo," *Institute for Defense and Government Advancement 3rd Annual Meeting*, Arlington, VA USA, March 1, 2005.

[18] R. K. Abercrombie, F. T. Sheldon, B. G. Schlicher, and K. M. Daley, "Development of the Joint Weigh-In-Motion and Measurement Reach Back Capability," *40th Annual International Logistics Conference 2005, Logistics: Product and Process for Capacity*, Orlando, Florida August 16, 2005.

[19] "Weigh-In-Motion Generation II," U.S. Army Deployment Process Modernization Office (DPMO) Quarterly Army Division Transportation Officer (DTO) & Mobility Officer (MO) Newsletter, Volume 1, Issue 1, p.5, May 20, 2005.

[20] R. K. Abercrombie. F. T. Sheldon, and B. G. Schlicher, "WIM Configuration and Data Management Activities," in *North American Travel Monitoring Exhibition & Conference*, Minneapolis, Minnesota, June 4-7, 2006.

[21] "Technologies for Troops: Getting There Faster" in *ORNL Review,* Volume 39, November 1, 2006, http://www.ornl.gov/info/ornlreview/v39_1_06/article08.shtml, (Last accessed January 30, 2008).

[22] R. K. Abercrombie, D. L. Beshears, L. M. Hively, M. B. Scudiere, F. T. Sheldon, J. L. Schmidhammer, J. Vanvactor, *ORNL/TM-2005/164,* "Prototype Weigh-In-Motion Performance", October 2006.

[23] D. Halliday and R. Resnick, Physics Parts I & II, John Wiley and Sons publ. (1966) pp.372-375.

[24] S.M. Selby and B. Girling, Standard Mathematical Tables, Chemical Rubber Company publ. (1965) pp. 410-413.

[25] See http://www.mathworks.com for details (Last accessed January 30, 2008).

[26] L.M. Hively and E.G. Ng, "Integrated Method for Chaotic Time Series Analysis," *U.S. Patent #5,815,413* (September 29. 1998).

[27] V. Protopopescu and L.M. Hively, "Phase-space Dissimilarity Measures of Nonlinear Dynamics: Industrial and Biomedical Applications," *Recent Res. Devel. Physics*, 6 (2005) 649-688.

Appendix A
TABLES AND FIGURES

APPENDIX A. TABLES AND FIGURES

Table 1. Time and motion study results

Weighing/Measuring Techniques	Min:Sec (with marking)	Min:Sec (no marking)	Personnel Required	% of Data With Human Errors
Static Scale/Tape Measure	7:38	4:48	3	9%
Wheel-Weight Scales/Tape Measure	7:46	4:52	7	14%
ORNL System	3:03	0:13	3	none found

Table 2. Percent error (16 vehicle configurations between 5,600 and 70,000 pounds)

Scale Type	*e*(total weight)	*e*(axle weight)
ORNL weigh in motion	0.62	1.12
In-ground, static scale	0.10	1.06
Portable, wheel-weight scales	0.36	0.51

Table 3. Mode parameters for wrecker 6 analysis (item 12 of table 2)

Mode #	A_j	ω_j/ω_f	φ_j	α_j	e (%)
1	95.2472	1	1.3313	-0.0012	0.2462
2	8.2832	4	5.0593	0.0045	0.2025
3	11.4213	8	1.0561	-0.0059	0.1830
4	3.7675	20	0.0386	0.0030	0.1749
5	0.7999	2	2.3204	0.0131	0.1708
6	3.4096	10	4.0906	-0.0010	0.1671
7	3.0701	14	4.9012	-0.0001	0.1637
8	0.6711	27	6.0528	0.0144	0.1602
9	7.2189	37	1.4365	-0.0191	0.1569
10	2.8293	48	2.7994	0.0013	0.1529
11	2.3573	52	2.4696	0.0042	0.1482
12	2.3815	76	0.9351	0.0029	0.1442
13	2.3125	96	1.2766	0.0025	0.1407
14	1.3846	88	5.0775	0.0090	0.1358
15	2.2760	140	3.4244	0.0043	0.1306
16	3.7129	45	1.8259	-0.0032	0.1265
17	1.9396	109	0.9431	0.0034	0.1232
18	2.6694	125	0.4254	-0.0007	0.1199
19	2.5489	114	6.2634	-0.0019	0.1174
20	1.6380	130	3.7027	-0.0011	0.1162
21	4.0992	147	2.7709	-0.0038	0.1108
22	1.3923	18	2.1252	0.0053	0.1079
23	1.2566	40	2.5187	0.0060	0.1052
24	2.0693	59	0.3155	0.0015	0.1019
25	4.9993	71	4.1603	-0.0191	0.0994
26	1.0477	69	4.2485	0.0010	0.0986
27	2.5581	66	0.9991	-0.0028	0.0959
28	1.5289	84	2.9550	0.0002	0.0943
29	0.8959	80	4.8833	0.0093	0.0910
30	0.8574	99	0.2253	0.0051	0.0898
31	1.5192	93	6.2437	0.0050	0.0859
32	2.6482	25	2.4241	-0.0043	0.0831
33	1.0965	126	1.2292	-0.0107	0.0828
34	2.1482	122	5.4300	0.0005	0.0790
35	1.3610	50	0.0882	0.0024	0.0768
36	4.7227	156	0.3636	-0.0097	0.0734
37	0.5681	5	3.9061	0.0112	0.0711
38	1.5955	16	5.9471	-0.0003	0.0690
39	0.3049	33	2.6040	0.0160	0.0663
40	0.8304	54	0.0677	0.0067	0.0641
41	2.5939	63	4.9764	-0.0064	0.0613
42	4.2213	90	5.7000	-0.0169	0.0579
43	0.6118	137	4.1081	0.0095	0.0552
44	1.4269	160	6.0996	0.0004	0.0527
45	1.0490	12	1.8679	-0.0012	0.0516
46	0.3870	22	1.4481	0.0103	0.0502
47	1.1237	82	0.7753	-0.0014	0.0489
48	0.8899	85	2.8206	-0.0087	0.0486
49	0.1512	95	2.7723	0.0132	0.0482
50	0.1643	83	5.9309	0.0049	0.0481
51	1.0832	77	4.3522	0.0016	0.0461
52	0.0857	107	3.5684	0.0191	0.0454

Table 4. Unfiltered error, e(u), and filtered error, e(n), in training sets

Dataset	*N*	*e*(u)	*e*(1)	*e*(2)	*e*(3)	*e*(*M*)	*M*
1) StrykerA421	185	1.895	0.367	0.281	0.270	0.076	61
2) StrykerA422	179	0.519	0.251	0.211	0.201	0.048	59
3) StrykerA423	121	1.470	0.255	0.240	0.229	0.055	40
4) StrykerA424	189	1.926	0.309	0.264	0.245	0.047	63
5) StrykerA425	181	1.531	0.356	0.259	0.253	0.052	60
6) StrykerA426	174	0.786	0.227	0.214	0.211	0.052	58
average	**172**	**1.355**	**0.294**	**0.245**	**0.235**	**0.055**	
7) Wrecker1	157	1.604	0.268	0.233	0.221	0.054	52
8) Wrecker2	157	0.966	0.370	0.214	0.182	0.037	52
9) Wrecker3	157	0.740	0.474	0.213	0.197	0.056	52
10) Wrecker4	157	0.320	0.253	0.224	0.210	0.045	52
11) Wrecker5	156	0.540	0.365	0.212	0.204	0.058	52
12) Wrecker6	157	0.974	0.246	0.203	0.183	0.039	52
average	**157**	**0.857**	**0.334**	**0.216**	**0.199**	**0.048**	
13 Suburban1	90	1.512	0.827	0.789	0.737	0.221	30
14)	89	1.470	0.980	0.951	0.913	0.228	29
15)	151	1.608	1.238	1.158	1.045	0.233	50
16) Suburban2	87	1.185	0.851	0.761	0.715	0.169	29
17)	91	1.093	0.952	0.866	0.834	0.188	30
18)	137	1.097	0.840	0.820	0.802	0.203	45
19) Suburban3	139	1.331	0.909	0.877	0.839	0.208	46
20) Suburban4	141	0.835	0.695	0.671	0.651	0.161	47
21) Suburban5	145	1.185	1.010	0.938	0.914	0.236	48
22) Suburban6	145	1.428	1.198	1.035	0.945	0.268	48
average	**122**	**1.274**	**0.950**	**0.887**	**0.840**	**0.211**	
23) SuburbanF1	42	1.793	1.456	1.236	1.129	0.210	13
24) SuburbanF2	40	3.436	1.770	1.477	1.321	0.411	13
25) SuburbanF3	41	5.787	3.191	2.858	1.991	0.592	13
26) SuburbanF4	45	2.292	1.576	1.422	1.088	0.235	15
27) SuburbanF5	37	5.400	3.406	2.420	2.243	0.582	12
28) SuburbanF6	43	1.673	1.281	1.068	0.912	0.216	14
average	**41**	**3.397**	**2.113**	**1.747**	**1.448**	**0.374**	

Table 5. Characterization of test datasets

	In-Ground Scale Weight (lbs)				Number of Data Sets			
Vehicle	axle 1	axle 2	axle 3	total	Normal	½" Bump	1" Bump	Total
F-250	4,520 4,490	2,890 2,910		7,410 7,400	16	5	6	27
Freightliner	11,040 10,960	4,300 4,350	3,900 3,930	19,240 19,240	17	6	9	32
Hummer	2,520 2,510	2,440 2,450		4,960 4,960	18	7	11	36
Silverado	2,780 2,770	1,870 1,870		4,650 4,640	18	6	9	33
Total Sets					69	24	35	128

Table 6. Mode-removal results for each wheel crossing of F-250 vehicle

Set #		1st wheel crossing		2nd wheel crossing		3rd wheel crossing		4th wheel crossing		Total
	Flags	*e*(min)	$\overline{w}$	*e*(min)	$\overline{w}$	*e*(min)	$\overline{w}$	*e*(min)	$\overline{w}$	$\overline{W}$
01	X	0.0673	2098	**0.1213**	1373	0.0442	2308	0.0616	1497	7276
02	X	0.0412	2153	0.0661	1336	0.0388	2245	0.0501	1477	7211
03		0.0493	2130	0.0464	1356	0.0351	2298	0.0468	1501	7285
04		0.0448	2128	0.0985	1372	**0.1283**	2275	0.0446	1493	7268
05		0.0728	2098	0.0646	1371	0.0453	2179	0.0640	1511	7159
06		0.0360	2154	0.0791	1369	0.0394	2237	0.0577	1474	7234
07	X	0.0573	2130	0.0484	1377	0.0387	2253	0.0508	1479	7239
08		0.0416	2143	0.0624	1386	0.0599	2250	0.0679	1487	7266
09	X	**0.1270**	2080	0.0586	1302	0.0333	2232	0.0594	1465	7079
10		0.0546	2064	0.0441	1361	0.0367	2291	0.0539	1497	7213
11	X	0.0661	2085	0.0638	1350	0.0421	2248	0.0564	1512	7195
12	X	0.0781	2118	0.0628	1385	0.0368	2247	0.0703	1499	7249
13	X	0.0397	2085	0.0438	1380	0.0296	2252	0.0470	1505	7222
15	S	0.0520	2088	0.0981	1340	0.0861	2283	0.0540	1516	7227
16	S	0.0559	2064	0.0673	1379	0.0414	2233	0.0543	1497	7173
17		0.0358	2057	0.0773	1367	0.0776	2216	0.0513	1492	7132
b1	X	**0.1333**	2131	0.0734	1445	0.0348	2366	0.0533	1568	7510
b2		0.0964	2167	**0.1209**	1401	0.0521	2364	0.0844	1583	7515
b3	S	**0.1554**	2159	0.0544	1411	0.0564	2265	**0.1401**	1571	7406
b4	S	0.0540	2099	**0.1738**	1412	0.0534	2370	0.0601	1576	7457
b5		**0.2039**	2180	0.0596	1459	0.0395	2313	0.0577	1570	7522
B1	X	0.0720	2481	0.0721	1074	0.0944	2758	0.0687	1335	7648
B2	S	0.0507	1850	**0.1336**	1404	0.0322	2006	0.0379	1466	6726
B3		0.0483	1751	**0.1108**	1313	0.0519	1988	0.0501	1500	6552
B4	X	0.0724	2301	**0.1205**	1395	0.0305	2379	**0.1136**	1472	7547
B5		0.0811	2377	**0.1112**	1324	0.0432	2465	0.0403	1468	7634
B6	X	0.0381	2127	0.0538	1379	0.0384	2180	0.0456	1482	7168
$\overline{w}$		0.0713	2115	0.0810	1376	0.0496	2273	0.0608	1490	7285
$\sigma/\overline{w}$			0.017		0.015		0.025		0.011	0.019

Table 7. Mode-removal results for each wheel crossing of freightliner truck

Set #		1st wheel crossing		2nd wheel crossing		3rd wheel crossing		4th wheel crossing		5th wheel crossing		6th wheel crossing		Total
	Flags	*e*(min)	$\overline{w}$	*e*(min)	$\overline{w}$	*e*(min)	$\overline{w}$	*e*(min)	$\overline{w}$	*e*(min)	$\overline{w}$	*e*(min)	$\overline{w}$	$\overline{W}$
01	X	0.0153	5390	0.0352	2156	**0.1149**	1984	0.0137	5545	0.0464	1952	0.0416	2004	19031
02	S	0.0490	5433	**0.1027**	2094	0.0554	1983	0.0163	5532	0.0395	1909	**0.1235**	1952	18903
03	S	0.0197	5229	0.0285	2117	0.0927	1977	0.0136	5410	0.0377	1951	**0.1270**	1959	18643
04	S	0.0140	5305	0.0831	2152	0.0489	2006	0.0138	5545	0.0404	1939	0.0761	2014	18961
05		0.0244	5297	0.0300	2161	**0.1194**	1975	0.0118	5539	0.0375	1888	**0.1257**	2021	18881
06	S	0.0172	5261	0.0298	2142	0.0901	1981	0.0521	5554	0.0345	1897	0.0400	1950	18785
07	S	0.0175	5409	0.0282	2191	0.0753	1970	0.0182	5507	**0.1403**	1892	0.0383	1906	18875
08	S	0.0134	5322	0.0301	2216	0.0355	1950	0.0127	5502	0.0410	1879	**0.1191**	2042	18911
09	S	0.0322	5328	0.0353	2170	**0.1522**	1929	0.0104	5519	0.0365	1856	0.0360	2024	18826
10	S	0.0154	5312	0.0844	2152	0.0314	1981	0.0210	5454	0.0386	1881	0.0322	2012	18792
11	S	0.0460	5278	0.0488	2146	0.0278	1970	0.0166	5426	0.1074	1886	0.0501	2011	18717
12	S	0.0379	5276	**0.1083**	2135	0.0390	1978	0.0167	5496	0.0292	1898	**0.1293**	1945	18728
13	S	0.0158	5340	0.0595	2193	0.0519	1992	0.0120	5492	0.0315	1867	0.0314	2007	18891
14	S	0.0371	5334	0.0321	2157	0.0346	1991	0.0478	5657	0.0636	1916	0.0560	1990	19045
15		0.0434	5433	0.0254	2128	0.0342	1982	0.0736	5651	**0.1100**	1901	**0.1243**	1930	19025
16	S	0.0172	5349	0.0238	2141	**0.1084**	1984	0.0146	5471	0.0353	1915	**0.1632**	1922	18782
17	S	0.0536	5335	0.0334	2124	0.0389	1978	**0.2025**	5575	0.0506	1943	0.0403	1930	18885
b1	S	0.0115	5283	0.0376	2166	0.0341	1956	0.0136	5401	0.0617	1901	**0.1159**	1918	18625
b2		0.0427	5328	0.0385	2144	**0.1105**	1997	0.0985	5658	0.0636	1998	**0.1378**	1911	19036
b3	S	0.0139	5253	0.0261	2119	**0.1630**	1943	0.0136	5378	0.0284	1984	0.0560	1944	18621
b4	X	0.0113	5118	0.0314	2118	0.0559	1959	**0.1394**	5713	0.0633	1915	**0.1173**	1959	18782
b5	S	0.0238	5165	0.0341	2088	0.0513	1959	0.0439	5550	0.0640	1965	**0.1002**	1917	18644
b6	S	0.0173	5126	0.0998	2105	0.0792	1961	0.0120	5494	0.0430	1926	0.0447	1954	18566
B1	S	0.0462	5326	0.0825	1970	**0.1457**	1943	0.0133	5432	**0.1074**	1690	**0.1040**	1964	18325
B2		0.0699	5152	**0.1419**	1895	**0.2471**	1983	0.0249	5246	**0.1219**	1638	**0.2095**	1900	17814
B3	X	0.0191	5439	**0.1622**	1910	**0.1104**	1984	0.0474	5245	**0.1881**	1614	**0.2452**	1898	18090
B4	S	0.0106	5328	**0.1343**	1867	0.0961	1948	0.0107	5330	**0.1186**	1668	0.0875	1910	18051
B5	S	0.0125	5292	**0.1002**	2164	0.0506	1951	0.0188	5497	0.0639	1939	**0.1094**	1943	18786
B6	X	0.0129	5308	**0.1240**	2150	**0.1195**	1951	0.0136	5430	0.0896	1980	**0.1026**	2023	18842
B7	S	0.0147	5358	**0.1209**	2097	0.0308	1973	0.0118	5472	**0.1173**	1945	0.0302	1965	18810
B8		0.0431	5189	0.0801	2056	0.0374	2011	0.0123	5460	0.0454	2013	0.0367	1901	18630
B9	S	0.0115	5206	**0.1056**	2069	0.0312	2039	0.0174	5506	0.0308	2041	0.0581	1918	18779
$\overline{w}$		0.0259	5324	0.0668	2140	0.0785	1971	0.0331	5492	0.0665	1917	0.0909	1958	18814
$\sigma/\overline{w}$			0.011		0.013		0.008		0.009		0.018		0.022	0.007

Table 8. Mode-removal results for each wheel crossing of hummer H3 vehicle

Set #		1st wheel crossing		2nd wheel crossing		3rd wheel crossing		4th wheel crossing		Total
	Flags	*e*(min)	$\overline{w}$	*e*(min)	$\overline{w}$	*e*(min)	$\overline{w}$	*e*(min)	$\overline{w}$	$\overline{W}$
01	X	0.0697	1153	0.0647	1162	0.0386	1299	0.0504	1201	4815
02	X	0.0614	1159	0.0919	1168	0.0516	1301	0.0950	1216	4844
03		0.0726	1155	**0.1162**	1186	0.0517	1312	0.0907	1220	4873
04		**0.1034**	1159	0.0974	1190	0.0529	1277	0.0719	1189	4815
05		**0.2472**	1143	0.0995	1197	**0.3332**	1286	0.0993	1207	4833
06	X	**0.1236**	1156	0.0968	1163	0.0580	1304	0.0943	1206	4829
07	S	**0.1397**	1173	**0.1123**	1170	0.0529	1300	0.0972	1202	4845
08		0.0976	1169	**0.1180**	1193	--	--	--	--	--
09	S	0.0716	1148	0.0592	1173	0.0570	1271	0.0713	1207	4799
10	S	0.0895	1188	**0.1080**	1173	0.0478	1292	0.0885	1197	4850
11		0.0725	1142	**0.1006**	1174	0.0404	1291	**0.1062**	1206	4813
12	S	**0.1308**	1163	**0.2510**	1207	0.0379	1262	0.0539	1185	4817
13		0.0705	1176	0.0818	1180	0.0461	1299	0.0662	1197	4852
14		0.0495	1175	0.0848	1185	0.0737	1289	0.0873	1199	4848
15	S	**0.1117**	1155	**0.1204**	1182	0.0652	1280	0.0765	1213	4830
16	S	0.0812	1159	0.0706	1193	0.0448	1295	0.0582	1195	4842
17	X	0.0842	1155	**0.1144**	1210	0.0668	1279	0.0690	1211	4855
18	S	0.0802	1170	0.0765	1186	0.0705	1311	0.0867	1228	4895
B01	S	**0.1011**	1147	0.0732	1156	0.0517	1282	0.0729	1162	4747
B02	S	0.0585	1150	0.0703	1144	0.0474	1307	0.0744	1182	4783
B03	S	0.0520	1149	0.0790	1134	0.0412	1296	0.0946	1225	4804
B04	S	0.0532	1167	0.0818	1158	0.0503	1276	**0.1030**	1189	4790
B05		0.0443	1167	0.0475	1177	0.0440	1265	0.0608	1163	4772
B06		0.0533	1151	0.0638	1145	0.0503	1272	0.0702	1176	4744
B07	S	0.0604	1142	0.0538	1155	0.0503	1245	0.0601	1199	4741
BB01	X	0.0592	1165	0.0521	1180	0.0931	1273	**0.1826**	1203	4821
BB02		**0.1968**	1136	0.0704	1180	0.0519	1272	0.0927	1220	4808
BB03		0.0592	1172	0.0545	1190	0.0451	1272	0.0768	1216	4850
BB04		**0.1389**	1144	0.0719	1164	**0.1315**	1390	0.0723	1209	4907
BB05	X	0.0560	1149	0.0923	1165	0.0462	1318	0.0987	1215	4847
BB06		**0.3820**	1165	**0.4614**	1372	--	--	--	--	--
BB07	S	0.0430	1169	0.0905	1173	0.0551	1339	0.0800	1204	4885
BB08	S	0.0864	1183	0.0557	1198	0.0493	1313	0.0491	1208	4902
BB09	S	0.0629	1177	0.0492	1299	--	--	--	--	--
BB10		**0.2846**	1167	**0.1329**	1191	**0.2888**	1340	0.0848	1199	4897
BB11		0.0591	1219	0.0743	1186	0.0841	1328	0.0947	1204	4937
$\overline{w}$		0.1002	1158	0.0983	1178	0.0718	1289	0.0827	1205	4839
$\sigma/\overline{w}$			0.010		0.011		0.012		0.007	0.007

Table 9. Mode-removal results for each wheel crossing of silverado vehicle

Set #		1st wheel crossing		2nd wheel crossing		3rd wheel crossing		4th wheel crossing		Total
	Flags	*e*(min)	$\overline{w}$	*e*(min)	$\overline{w}$	*E*(min)	$\overline{w}$	*e*(min)	$\overline{w}$	$\overline{W}$
01		**0.1241**	1310	**0.1800**	877	0.0512	1365	0.0575	937	4489
02	S	**0.1397**	1288	**0.1488**	891	0.0495	1395	0.0559	924	4498
04	S	0.0725	1280	0.0941	884	0.0478	1389	0.0520	935	4488
05	X	0.0525	1283	0.0891	898	0.0388	1395	0.0508	930	4506
06		0.0580	1268	0.0735	877	0.0513	1408	0.0697	945	4498
07		0.0566	1272	0.0829	868	0.0430	1399	0.0695	946	4485
08	S	0.0791	1285	0.0772	889	0.0420	1403	0.0634	926	4503
10	X	**0.1109**	1283	0.0940	909	0.0592	1400	0.0736	917	4509
11	X	0.0645	1289	0.0815	875	0.0522	1402	0.0751	937	4503
12	S	0.0736	1269	0.0741	885	0.0545	1416	0.0744	932	4502
13		0.0624	1316	0.0771	927	0.0806	1401	0.0577	932	4576
14		0.0549	1291	0.0873	878	0.0489	1403	0.0693	943	4515
15	S	0.0560	1293	0.0575	895	0.0566	1399	0.0625	916	4503
16	S	0.0780	1272	**0.1073**	892	0.0551	1380	0.0843	939	4483
17	S	**0.1071**	1286	0.0631	896	0.0496	1382	0.0584	935	4499
18		0.0599	1315	0.0864	920	0.0373	1376	0.0745	901	4512
19	X	0.0580	1285	0.0717	894	0.0507	1397	0.0749	935	4511
20	S	0.0876	1314	0.0907	910	0.0391	1386	0.0579	924	4534
B01		0.0816	1363	0.0888	922	0.0594	1470	0.0558	943	4698
B02		0.0910	1375	0.0790	904	0.0445	1448	0.0597	956	4683
B03		0.0768	1366	0.0627	900	0.0487	1461	0.0723	939	4666
B04		0.0782	1363	0.0643	907	0.0435	1455	0.0727	953	4678
B05	S	0.0865	1354	0.0819	925	0.0489	1412	0.0861	923	4614
B06	X	0.0935	1326	0.0743	906	0.0485	1459	0.0693	931	4622
BB01		0.0645	1148	0.0709	787	0.0502	1249	0.0581	948	4132
BB02	S	**0.1029**	1121	0.0902	802	0.0361	1231	0.0693	931	4085
BB03	S	0.0648	1274	**0.1226**	845	0.0741	1366	0.0645	939	4424
BB04		0.0438	1328	0.0801	919	0.0445	1412	0.0661	913	4572
BB05		0.0599	1132	0.0957	797	0.0614	1213	0.0691	939	4081
BB06	X	**0.1008**	1260	**0.1243**	885	0.0463	1327	0.0680	934	4406
BB07	S	0.0969	1304	0.0743	876	0.0412	1393	0.0544	934	4507
BB08		**0.1063**	1250	0.0867	882	**0.1086**	1320	0.0687	934	4386
BB09		0.0385	1319	0.0891	918	0.0375	1392	0.0562	913	4542
$\overline{w}$		0.0782	1290	0.0885	897	0.0515	1397	0.0658	935	4501
$\sigma/\overline{w}$			0.016		0.019		0.008		0.007	0.002

Table 10. Occurrence rate of error below 0.1% for single-wheel-crossing data

Vehicle Name	Normal (# Sets)	½" Bump (# Sets)	1" Bump (# Sets)
F-250	**61/64 = 95%**	14/20 = 70%	19/24 = 79%
Freightliner	**86/102 = 84%**	29/36 = 81%	33/54 = 61%
Hummer	54/70 = 77%	**26/28 = 93%**	31/40 = 78%
Silverado	65/72 = 90%	**24/24 = 100%**	30/36 = 83%
Totals	266/308 = 86%	**93/108 = 91%**	113/154 = 73%

Table 11. Occurrence rate of outliers for single-wheel-crossing data

Vehicle Name	Normal (# Sets)	½" Bump (# Sets)	1" Bump (# Sets)
F-250	1/64 = 2%	7/20 = 35%	13/24 = 54%
Freightliner	5/102 = 5%	7/36 = 19%	19/54 = 35%
Hummer	5/70 = 7%	9/28 = 32%	8/40 = 20%
Silverado	4/72 = 6%	12/24 = 50%	15/36 = 42%
Totals	15/308 = 5%	35/108 = 32%	55/154 = 36%

Table 12. Comparison of IGS and WIM from single-wheel crossings (pounds)

	In-Ground Scale Weight				WIM Weight			
Vehicle	axle 1	axle 2	axle 3	Total	axle 1	axle 2	axle 3	Total
F-250	4,520	2,890		7,410	4,377	2,868		7,285
	4,490	2,910		7,400	(65)	(10)		(137)
Freightliner	11,040	4,300	3,900	19,240	10,790	4,060	3,932	18,814
	10,960	4,350	3,930	19,240	(108)	(30)	(45)	(136)
Hummer	2,520	2,440		4,960	2,447	2,384		4,839
	2,510	2,450		4,960	(20)	(15)		(36)
Silverado	2,780	1,870		4,650	2,684	1,823		4,501
	2,770	1,870		4,640	(10)	(9)		(10)

Table 13. Mode-removal results for each axle of F-250 vehicle

Set #	1st axle		2nd axle		Total
	e(min)	$\overline{w}$	*e*(min)	$\overline{w}$	$\overline{W}$
01	0.0431	4305	0.0563	2878	7183
02	0.0321	4398	0.0410	2823	7221
03	0.0263	*4450*	0.0415	2858	*7308*
04	0.0453	4389	0.0342	2844	7233
05	**0.1250**	4287	0.0402	2838	7125
06	0.0439	4369	0.0491	2849	7218
07	0.0321	4360	0.0271	2864	7224
08	0.0352	4375	0.0544	2871	7246
09	0.0280	4376	0.0507	*2754*	7130
10	0.0334	4335	0.0368	2867	7202
11	0.0255	4338	0.0417	2849	7187
12	0.0370	4340	0.0458	2891	7231
13	0.0284	4325	0.0352	2887	7212
15	0.0319	4367	0.0351	2819	7186
16	0.0248	4305	0.0431	2836	7141
17	0.0314	*4253*	0.0597	2827	*7080*
b1	0.0628	4522	0.0508	2990	7512
b2	0.0922	4512	0.0552	2985	7497
b3	0.0432	4429	0.0366	2976	7405
b4	0.0235	4455	0.0429	2962	7417
b5	0.0254	4468	0.0469	2998	7466
B1	0.0908	5295	0.0613	2377	7672
B2	0.0308	3761	0.0732	2875	6636
B3	0.0241	3850	0.0360	2789	6639
B4	0.0575	4732	0.0650	2838	7570
B5	0.0508	4677	0.0452	2776	7453
B6	0.0242	4249	0.0263	2894	7143
$\overline{\overline{w}}$	0.0425	4373	0.0456	2871	7262
$\sigma/\overline{\overline{w}}$		0.017		0.023	0.018

Table 14. Mode-removal results for each axle of freightliner truck

Set #	1st axle		2nd axle		3rd axle		Total
	e(min)	$\overline{w}$	*e*(min)	$\overline{w}$	*e*(min)	$\overline{w}$	$\overline{W}$
01	0.0169	10984	0.0260	4064	0.0308	4010	19058
02	0.0092	11113	0.0292	4015	0.0569	3938	19066
03	0.0152	10690	0.0288	4027	0.0428	3910	18627
04	0.0104	10916	0.0243	4061	**0.1282**	3961	18938
05	0.0159	10909	0.0779	4042	**0.1128**	3916	18867
06	0.0085	10819	0.0647	4036	0.0872	3914	18769
07	0.0287	10907	0.0714	4083	0.0754	3927	18917
08	0.0118	10827	0.0623	4006	0.0263	3898	18731
09	0.0060	10813	0.0813	4016	0.0265	3885	18714
10	0.0321	10754	0.0314	4033	0.0734	3907	18694
11	0.0077	10709	0.0301	4087	0.0793	3949	18745
12	0.0077	10788	0.0194	4038	0.0227	3904	18730
13	0.0073	10811	0.0790	4049	0.0319	3930	18790
14	0.0093	10969	0.0311	4096	0.0515	3923	18988
15	0.0557	11062	0.0432	4039	0.0279	3914	19015
16	0.0095	10865	0.0272	4061	0.0233	3904	18830
17	0.0543	10958	0.0267	4069	0.0528	3896	18923
b1	0.0096	10839	0.0464	4068	0.0871	3866	18773
b2	0.0082	10798	0.0384	4135	0.0946	3922	18855
b3	0.0670	10933	0.0518	4148	0.0889	3874	18955
b4	0.0095	10615	0.0251	4041	0.0254	3879	18535
b5	0.0090	10395	0.0260	4031	0.0831	3889	18315
b6	0.0085	10518	0.0524	4019	0.0277	3892	18429
B1	0.0864	10655	**0.1097**	3664	0.0393	3874	18193
B2	0.0087	10570	**0.1436**	3467	0.0952	3876	17913
B3	0.0288	10533	0.0570	3464	0.0286	3877	17874
B4	0.0066	10636	0.0269	3498	0.0891	3869	18003
B5	0.0108	10719	0.0264	4096	0.0230	3889	18704
B6	0.0078	10831	0.0852	4067	0.0301	3881	18779
B7	0.0092	10763	0.0723	4112	0.0342	3880	18755
B8	0.0079	10720	0.0271	4073	0.0253	3854	18647
B9	0.0164	10714	**0.1172**	4037	0.0205	3872	18623
$\overline{\boldsymbol{w}}$	0.0188	10805	0.0519	4050	0.0544	3895	18809
$\boldsymbol{\sigma}/\overline{\boldsymbol{w}}$		0.010		0.006		0.006	0.008

Table 15. Mode-removal results for each axle of Hummer H3 vehicle

Set #	1st axle		2nd axle		Total
	e(min)	$\overline{w}$	*e*(min)	$\overline{w}$	$\overline{W}$
01	0.0395	2453	0.0516	2379	4832
02	0.0301	2471	0.0748	2368	4839
03	0.0414	2473	0.0670	2418	4891
04	0.0567	2429	0.0743	2359	4788
05	**0.3719**	2426	0.0671	2425	4851
06	0.0650	2462	0.0685	2370	4832
07	0.0761	2472	0.0731	2385	4857
08	0.0470	2396	--	--	
09	0.0394	2421	0.0494	2347	4768
10	0.0719	2476	0.0618	2374	4850
11	0.0357	2440	0.0595	2381	4821
12	**0.1027**	2427	0.0419	2382	4809
13	0.0353	2488	0.0422	2408	4896
14	**0.1176**	2450	0.0387	2385	4835
15	0.0670	2441	0.0670	2400	4841
16	0.0446	2453	0.0489	2381	4834
17	0.0513	2438	0.0594	2418	4856
18	**0.1185**	2476	0.0478	2410	4886
B01	0.0707	2451	0.0422	2317	4768
B02	0.0349	2463	0.0495	2309	4772
B03	0.0305	2423	0.0469	2359	4782
B04	0.0522	2445	0.0821	2359	4804
B05	0.0285	2405	0.0452	2355	4760
B06	0.0378	2437	0.0498	2328	4765
B07	0.0311	2403	0.0489	2365	4768
BB01	0.0329	2448	0.0591	2383	4831
BB02	0.0370	2416	0.0453	2397	4813
BB03	0.0368	2431	0.0454	2416	4847
BB04	**0.1073**	2529	0.0466	2369	4898
BB05	0.0275	2494	0.0425	2372	4866
BB06	**0.4509**	2544	--	--	
BB07	0.0799	2497	0.0482	2367	4864
BB08	0.0426	2506	0.0324	2399	4905
BB09	0.0431	2483	--	--	
BB10	**0.2628**	2515	0.0716	2396	4911
BB11	0.0494	2527	0.0621	2381	4908
$\overline{w}$	0.0797	2450	0.0549	2382	4835
$\sigma/\overline{w}$		0.012		0.008	0.010

Table 16. Mode-removal results for each axle of Silverado vehicle

Set #	1st axle		2nd axle		Total
	e(min)	$\overline{w}$	*e*(min)	$\overline{w}$	$\overline{W}$
01	0.0632	2654	**0.1115**	1818	4472
02	0.0697	2671	0.0907	1817	4488
04	0.0552	2674	0.0471	1811	4485
05	0.0632	2667	0.0466	1821	4488
06	0.0638	2655	0.0553	1835	4490
07	0.0546	2688	0.0578	1813	4501
08	0.0408	2687	0.0715	1811	4498
10	0.0490	2664	**0.1004**	1825	4489
11	0.0407	2670	0.0566	1816	4486
12	0.0400	2692	0.0496	1829	4521
13	0.0406	2715	0.0488	1837	4552
14	0.0379	2673	0.0583	1829	4502
15	0.0360	2677	0.0458	1825	4502
16	0.0327	2668	0.0439	1822	4490
17	0.0603	2669	0.0509	1816	4485
18	0.0358	2688	0.0556	1814	4502
19	0.0365	2682	0.0479	1822	4504
20	0.0638	2690	0.0623	1834	4524
B01	0.0488	2831	0.0531	1892	4723
B02	0.0471	2840	0.0450	1833	4673
B03	0.0429	2827	0.0421	1828	4655
B04	0.0389	2824	0.0564	1828	4652
B05	0.0448	2734	0.0418	1824	4558
B06	0.0361	2846	0.0414	1847	4693
BB01	0.0375	2420	0.0365	1777	4197
BB02	0.0355	2370	0.0459	1731	4101
BB03	0.0405	2593	0.0626	1792	4385
BB04	0.0278	2735	0.0396	1827	4562
BB05	0.0601	2341	0.0513	1757	4098
BB06	0.0551	2513	0.0575	1828	4341
BB07	0.0459	2675	0.0396	1808	4483
BB08	0.0590	2568	0.0489	1817	4385
BB09	0.0254	2703	0.0571	1825	4528
$\overline{\overline{w}}$	0.0463	2675	0.0551	1823	4493
$\sigma/\overline{\overline{w}}$		0.004		0.004	0.002

Table 17. Occurrence rate of error below 0.1% for single-axle data

Vehicle Name	Normal (# Sets)	½" Bump (# Sets)	1" Bump (# Sets)
F-250	31/32 = 97%	**10/10 = 100%**	**12/12 = 100%**
Freightliner	49/51 = 96%	**18/18 = 100%**	24/27 = 89%
Hummer	31/35 = 89%	**14/14 = 100%**	17/20 = 85%
Silverado	34/36 = 94%	**12/12 = 100%**	**18/18 = 100%**
Totals	145/154 = 94%	**54/54 = 100%**	71/77 = 92%

Table 18. Occurrence rate of outliers for single-axle data

Vehicle Name	Normal (# Sets)	½" Bump (# Sets)	1" Bump (# Sets)
F-250	0/32 = **0%**	0/10 = **0%**	6/12 = 50%
Freightliner	5/51 = **10%**	4/18 = 22%	7/27 = 26%
Hummer	1/35 = **7%**	3/14 = 21%	4/20 = 20%
Silverado	1/36 = **3%**	8/12 = 67%	11/18 = 61%
Totals	7/154 = **5%**	35/54 = 32%	55/77 = 36%

Table 19. Comparison of IGS and WIM for single-axle data (pounds)

	In-Ground Scale (IGS) Weight				WIM Weight			
Vehicle	axle 1	axle 2	axle 3	Total	axle 1	axle 2	axle 3	Total
F-250	4,520	2,890		7,410	4,373	2,871		7,262
	4,490	2,910		7,400	(74)	(66)		(131)
Freightliner	11,040	4,300	3,900	19,240	10,805	4,050	3,895	18,809
	10,960	4,350	3,930	19,240	(105)	(26)	(22)	(141)
Hummer	2,520	2,440		4,960	2,450	2,382		4,835
	2,510	2,450		4,960	(29)	(19)		(46)
Silverado	2,780	1,870		4,650	2,675	1,823		4,493
	2,770	1,870		4,640	(11)	(9)		(8)

Table 20. Whole-vehicle, mode-removal results for F-250 vehicle

Set #	$e(u)$ %	e(min) %	$\overline{W}$
01	0.2199	0.0297	7098
04	0.6109	0.0492	7174
05	0.6580	0.0537	6935
06	0.8496	0.0458	6915
07	0.6226	0.0354	7107
08	0.4773	0.0453	7117
11	0.1439	0.0214	6973
15	0.2426	0.0479	6935
17	0.5013	0.0411	7195
18	0.4303	0.0438	6927
19	0.3411	0.0382	6987
20	0.4404	0.0573	6820
21	0.7406	0.0371	6909
23	0.2528	0.0346	6990
28	0.6265	0.0445	7074
31	0.4022	0.0427	6881
32	0.5088	0.0376	6865
33	0.5655	0.0517	6881
34	0.4377	0.0374	6879
35	1.1327	0.0447	6809
mean	0.5102	0.0425	6974
$\sigma/\overline{w}$			0.017
IGS			7279±3

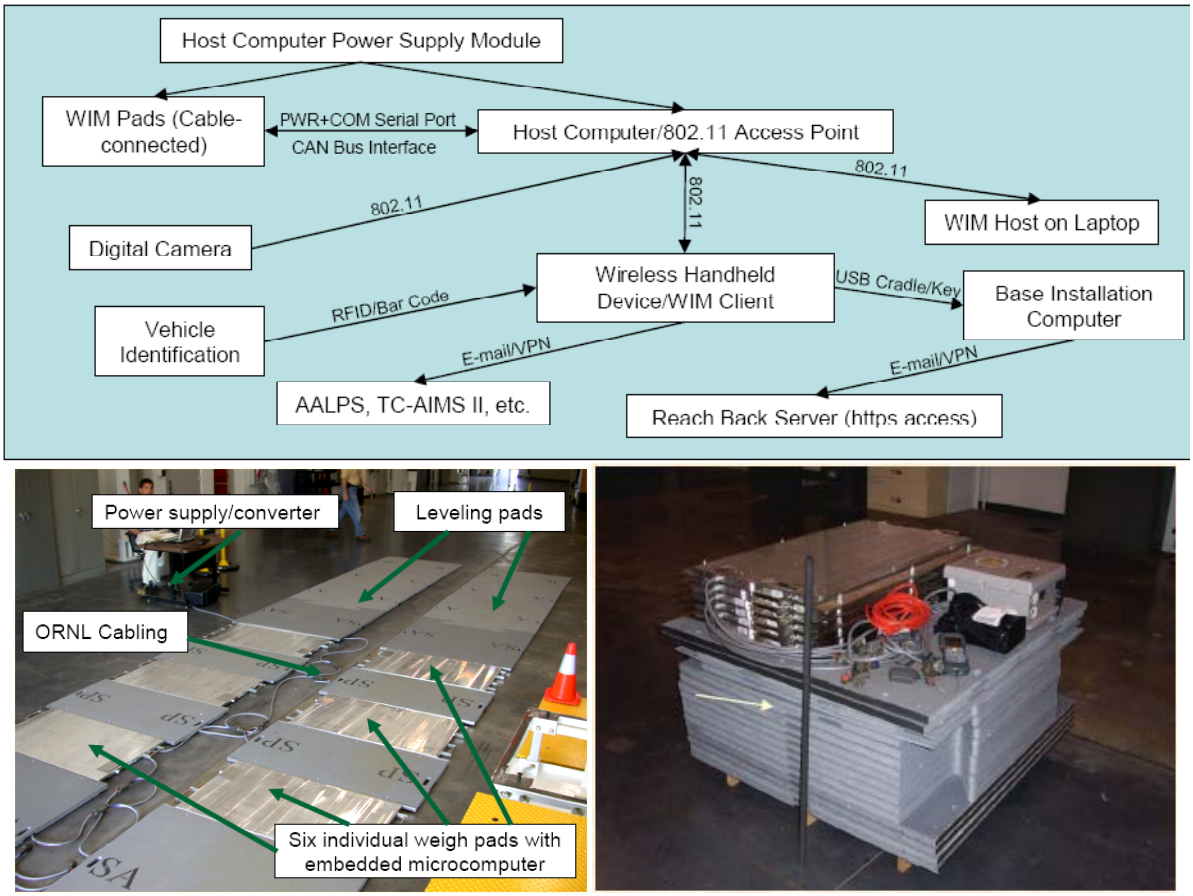

Figure 1. Weight measurement components and communication interfaces.

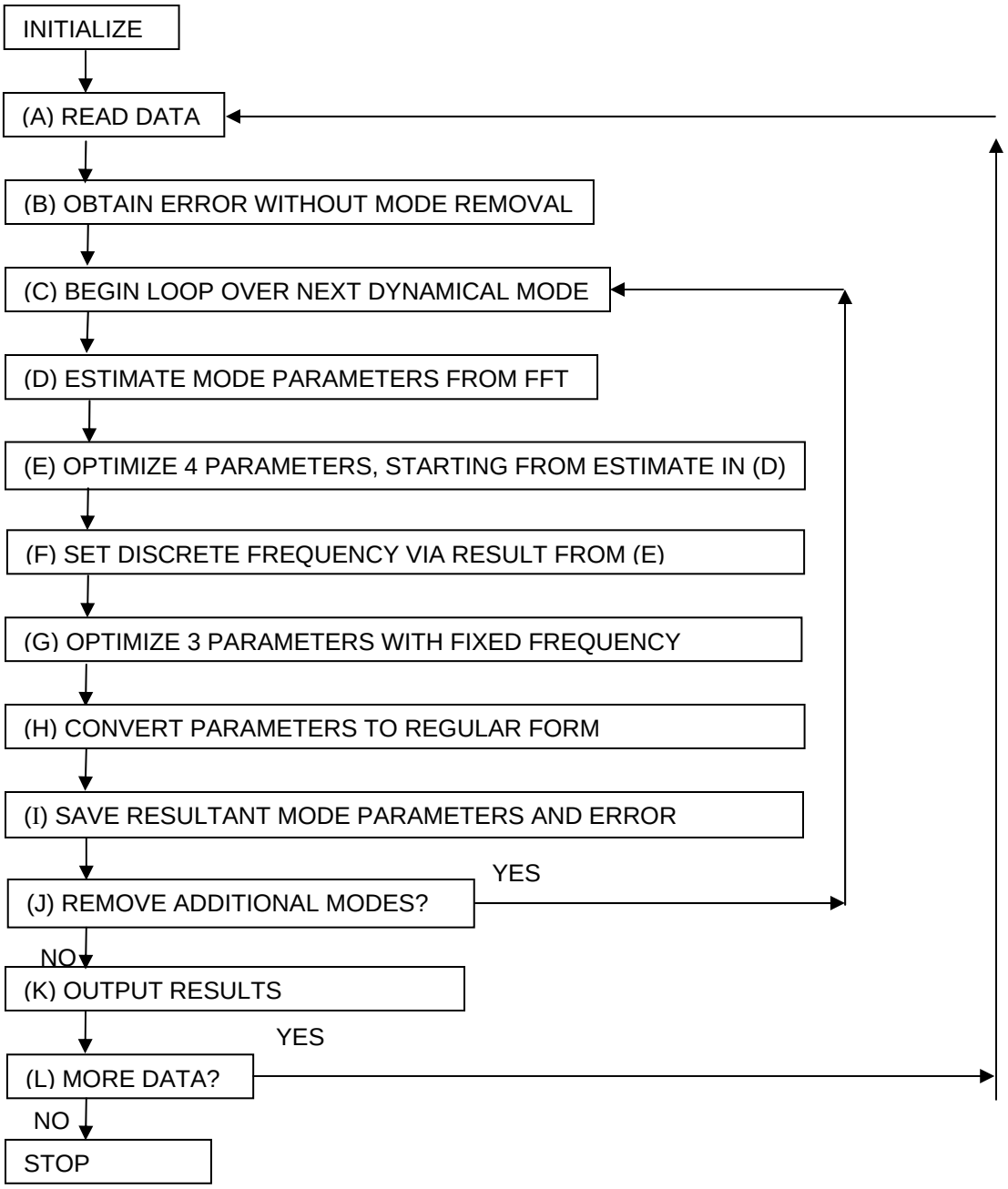

Figure 2. Flow diagram for nonlinear analysis. The letters in each box refer to the corresponding description in the text of Sect. 3.

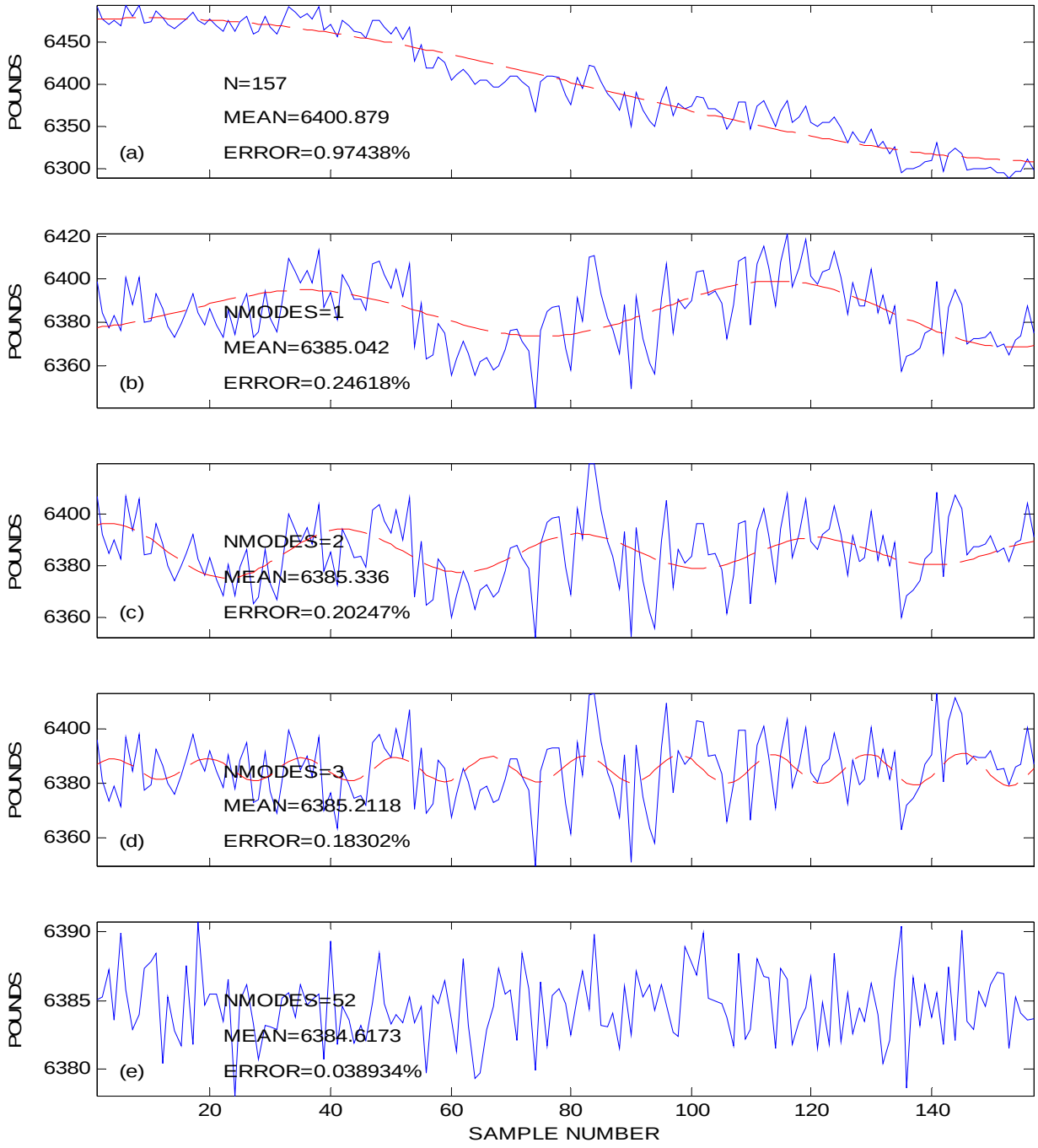

Figure 3. Time-serial weight measurements versus time (weight sample number, *i*) for (a) the unfiltered (raw) weight data (solid, blue curve) and the first oscillatory mode that the filtering method determined as the best low-order fit to the data (dashed, red curve), also showing the number of data points (N=157), mean weight value (MEAN), and resultant (unfiltered) measurement error (ERROR); (b) the residual weight (solid, blue curve) after removal of the first oscillatory mode (NMODES=1) from subplot (a), and the second oscillatory mode (dashed, red curve) that is removed with the corresponding mean and error. In the same fashion, subsequent subplots (c) – (d) show the resultant residual weight after removal of the previous mode(s) and the next oscillatory mode that is removed with the corresponding mean and error. Subplot (e) shows the residual time variation, mean, and error after removal of all (52) modes.

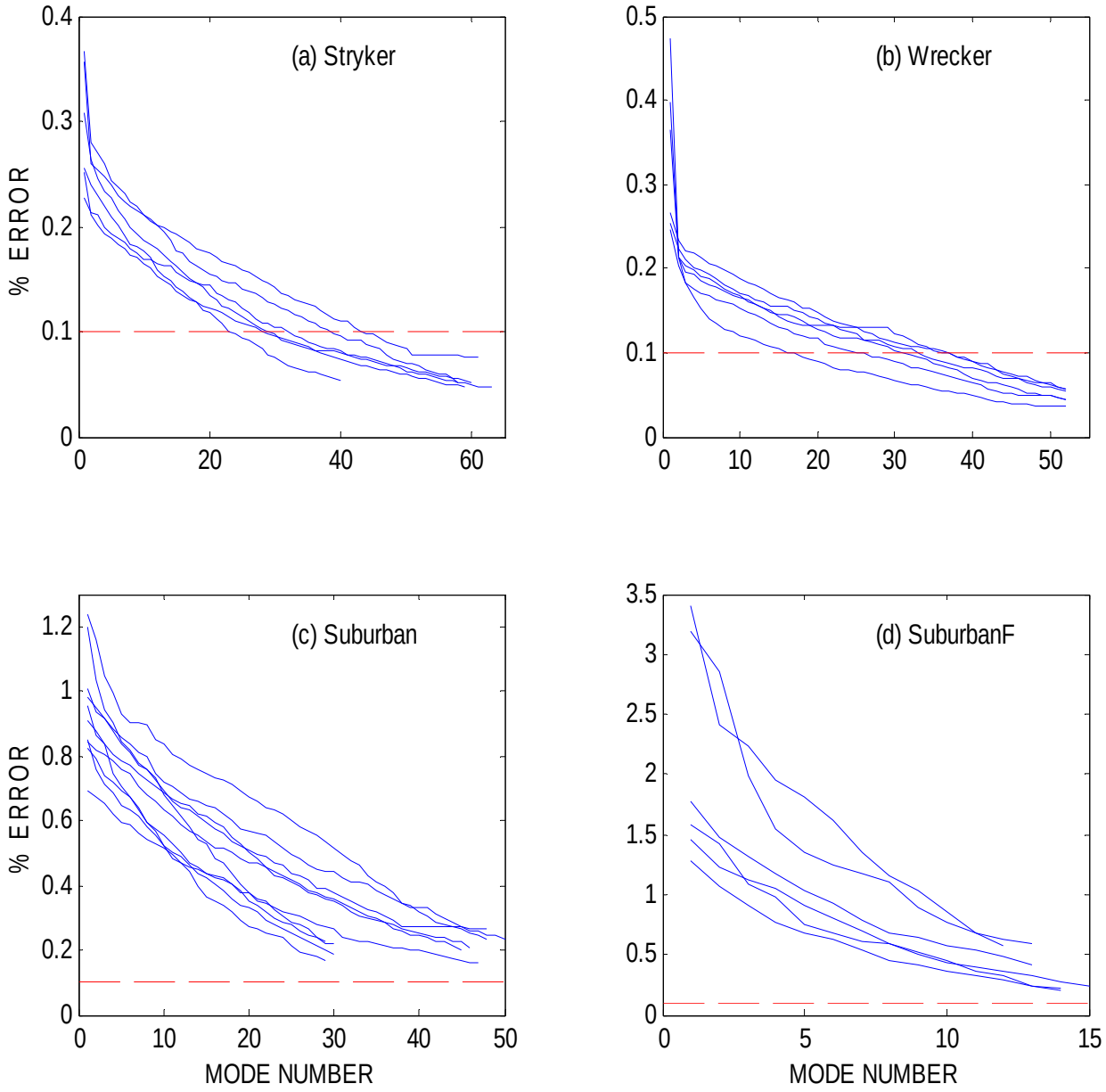

Figure 4. Decrease in residual (filtered) WIM error versus mode number for each of the four vehicle series in comparison to the 0.1% error limit for certifiable weights (dashed red line): (a) Stryker armored vehicle, (b) military wrecker vehicle, (c) unloaded Suburban, and (d) Suburban with 200 pounds of load.

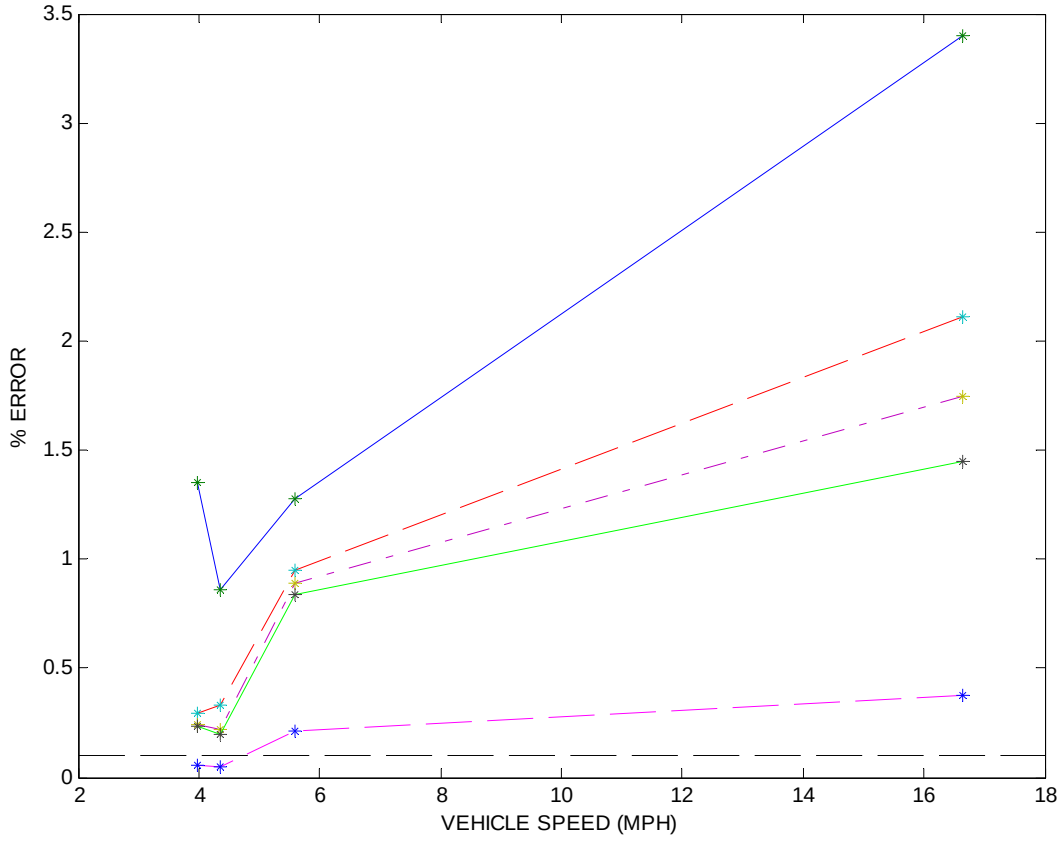

Figure 5. Average percent error in the WIM vehicle weight versus vehicle speed. Each curve shows error values from a column of Table 2, as follows: solid blue curve for no mode filtering, $e(u)$; dashed red curve(- -) for removal of one mode, $e(1)$ in Table 2; purple chain-dashed curve (-.-) for removal of two modes, $e(2)$ in Table 2; solid green curve for removal of three modes, $e(3)$ in Table 2; and dashed magenta curve (- -) for removal of M modes, $e(M)$ in Table 1. The horizontal black dashed curve (- -) indicates the 0.1% error level for certifiable weight measurements.

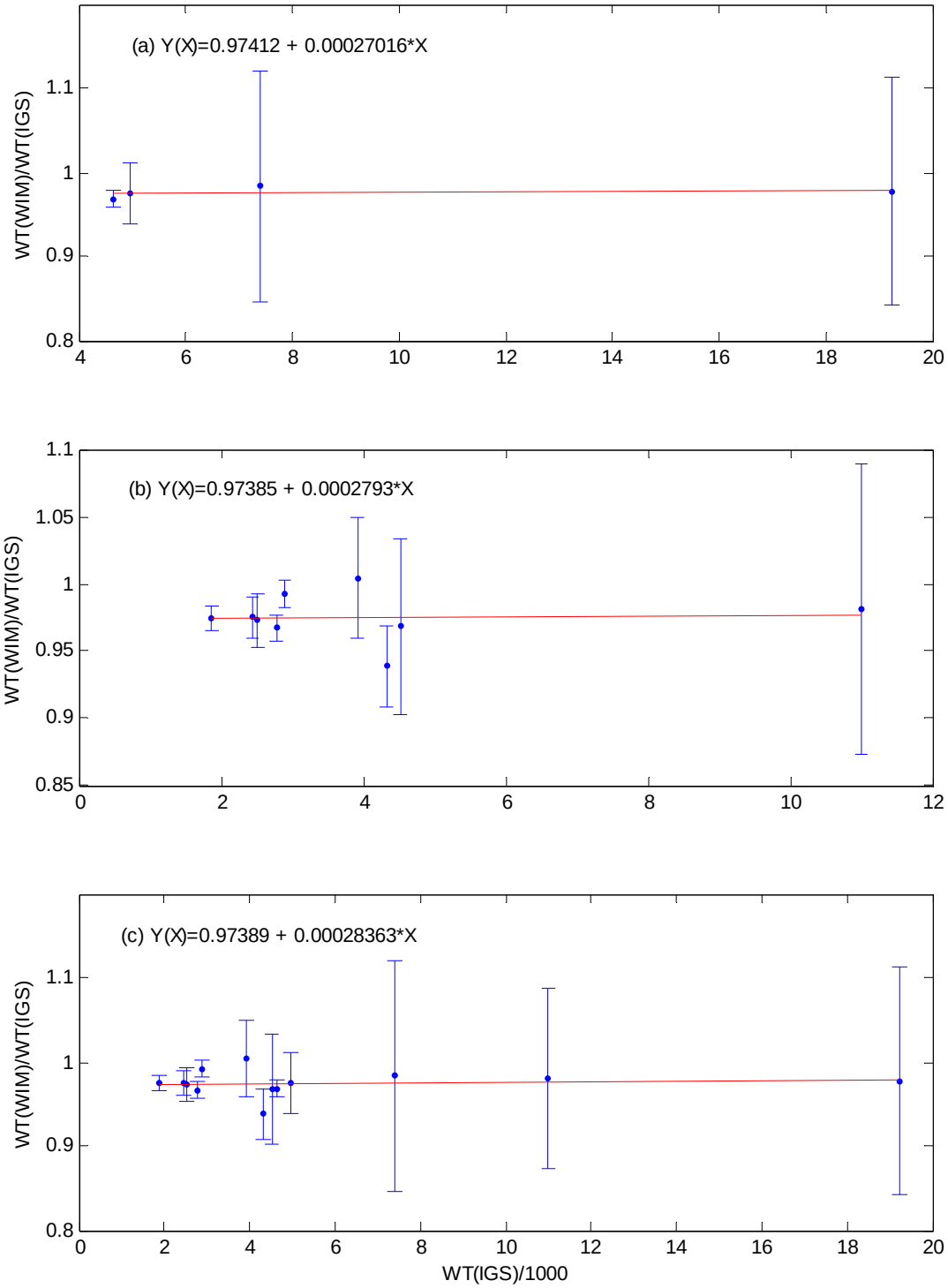

Figure 6. (WIM weight)/(IGS weight) versus IGS weight for (a) total weights, (b) single-axle weights, and (c) combination of (a) and (b). Straight-line fits for each set of data is shown for reference, along with the corresponding fitting parameters.

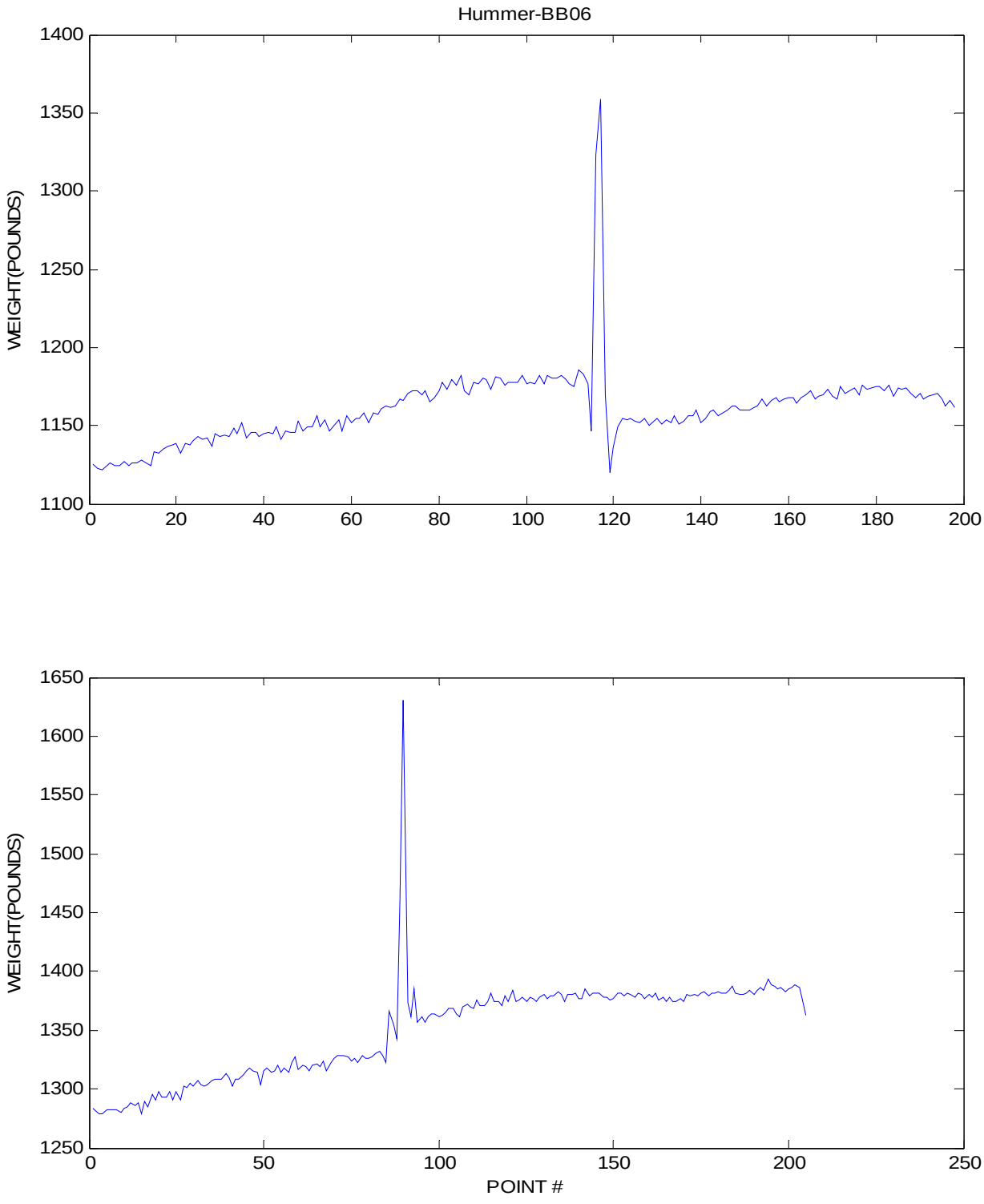

Figure 7. Raw Weight Data for Hummer-BB06 Dataset (see text for discussion).

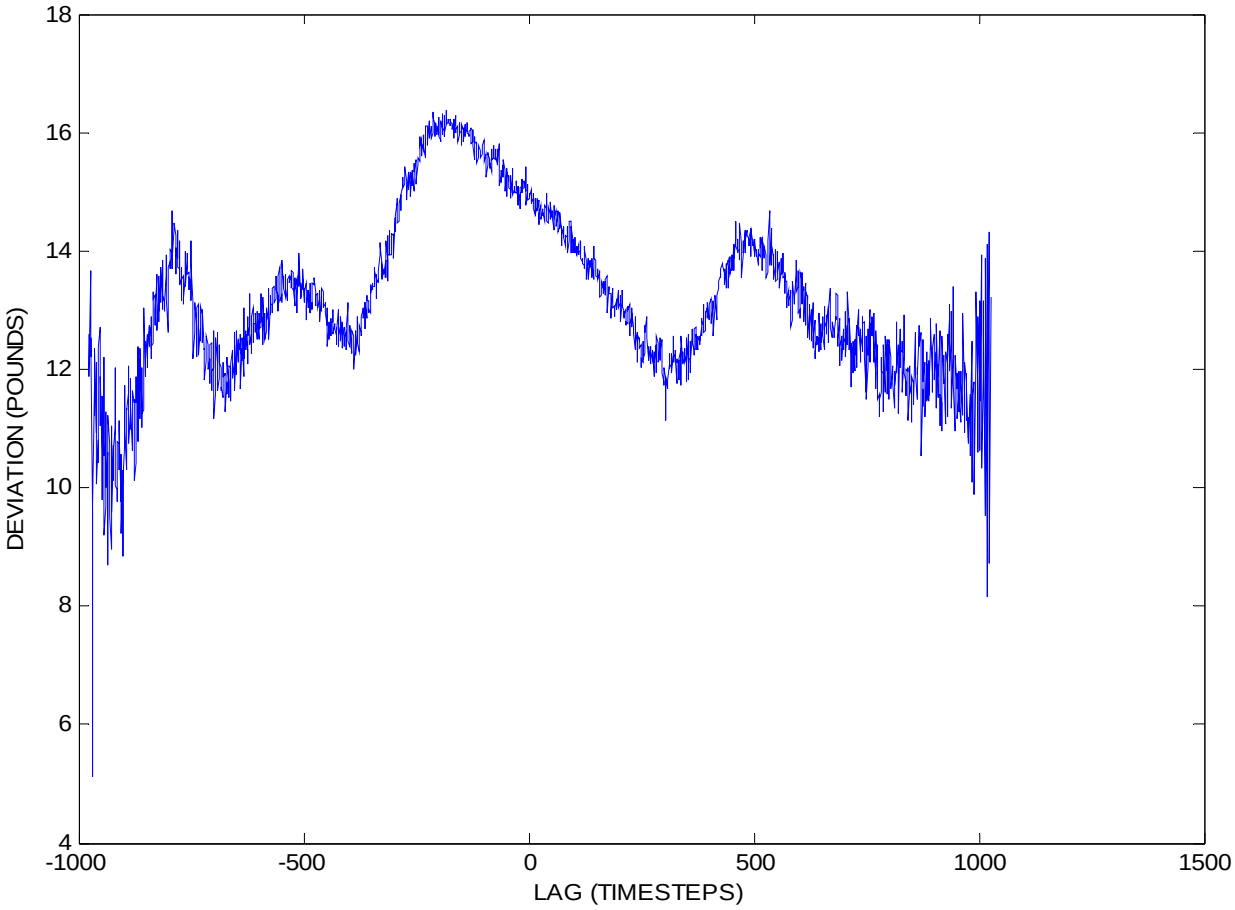

Figure 8. Sample standard deviation in the total WIM weight versus the time lag between the front- and rear-axle datasets for the Caravan-02 dataset without any clear minimum. See text for discussion.

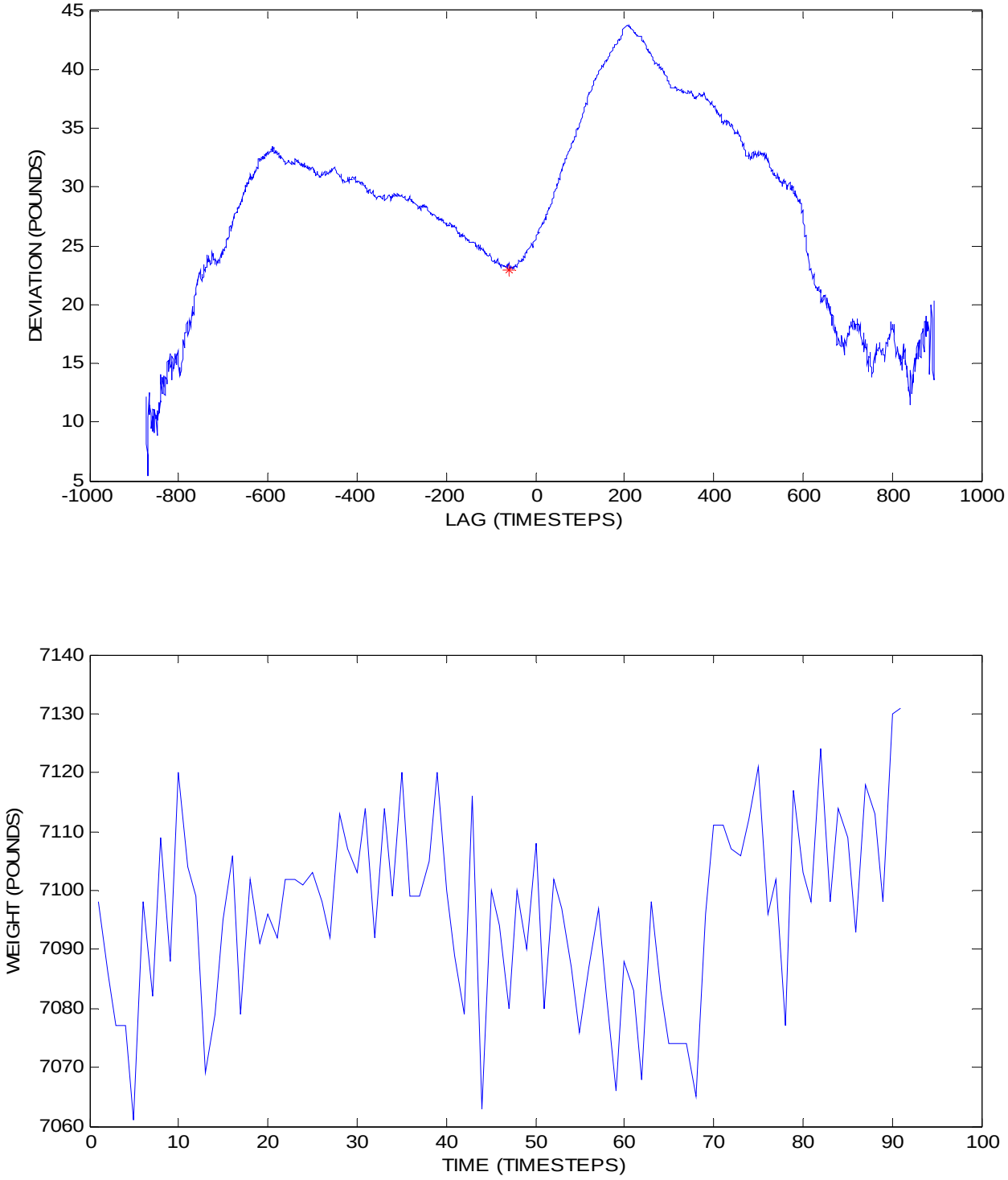

Figure 9. Sample standard deviation in the total WIM weight versus the time lag between the front- and rear-axle datasets for the F250-01 dataset with a clear minimum (red star in top plot) between two strong maxima; resultant total-vehicle weight versus time for the time-lag (bottom plot). See text for discussion.

Appendix B
MATHEMATICAL DETAILS OF WIM ANALYSIS

APPENDIX B: MATHEMATICAL DETAILS OF WIM ANALYSIS

This appendix describes the mathematical details of the WIM analysis to obtain the spacing of the vehicle axles for determination of the longitudinal center of balance. This analysis relies on discrete measurements as each wheel of the vehicle passes over the weigh pads. The specific measurements are the wheel weight and the time that the wheel is at the center (wheel-on-center time) of the weigh pad along with the speed of the wheel when it is on the center of the pad.

Some mathematical notation must first be defined. The weigh pads (WP) are labeled with the index, i, as shown in Figure B-1. The systematic placement of the numbers is shown for clarity, but may generally be in any arbitrary order. Six weigh pads are shown in the example of Figure B-1, but up to eight weigh pads are allowed by the present WIM software. The position of the i-th weigh pad along the direction of travel is denoted as D_i, and is fixed by the interlocking assembly with the spacing pads (SP), spacer-approach (SA) pads, and approach pads (AP).

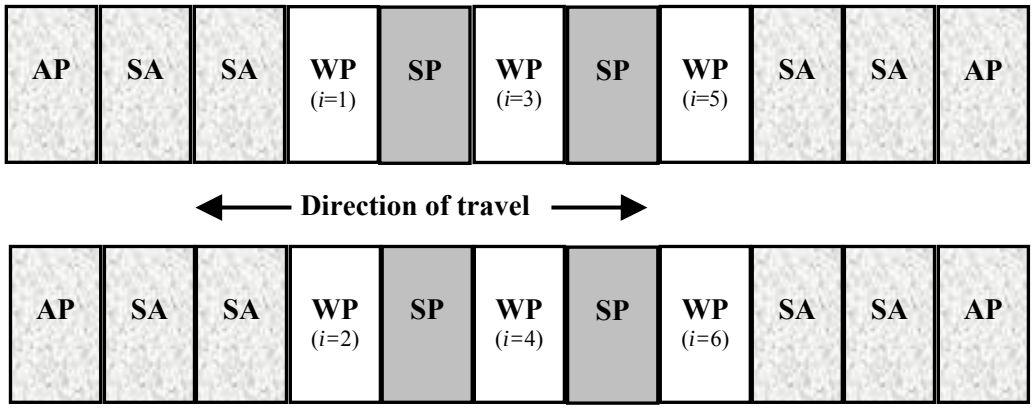

Figure B-1. Labeling of *i*-th weigh pads.

The vehicle axles are labeled with the index, j. Then, $j = 1$ labels the first (front) axle; $j = 2$ labels the second axle, and so on to the last (rear-most) axle. The position of the j-th axle along the vehicle length is then denoted as A_j.

One set of pads can be shifted along the direction of travel, relative to the other set. This shift is denoted by S, and applies to the right side (relative to the left side), as viewed from a vehicle moving along the direction of travel. This choice of "sides" is labeled by the index, k. Namely, $k = 0$ labels the left side, and $k = 1$ labels the right side. These definitions facilitate the subsequent mathematical description.

The weigh pad measurements are used to determine the vehicle position, as follows. The wheel-on-center location (x_{ijk}) is at the i-th pad for the j-th axle on the k-th side:

$$x_{ijk} = D_i + A_j + S \times k \,. \tag{B.1}$$

The corresponding time of this position measurement is t_{ijk}, for which the mathematical notation is:

$$x\left(t_{ijk}\right) = x_{ijk} \,. \tag{B.2}$$

The vehicle has a large momentum, and thus has a smoothly varying speed, so that higher order derivatives can be ignored without loss of accuracy. Therefore, this analysis assumes that the vehicle position can be approximated by a low-order polynomial function of time:

$$x\left(t_{ijk}\right) \approx \sum_{n=0}^{m} a_n t_{ijk}^{n} \,. \tag{B.3}$$

The symbol, Σ, denotes a summation over the polynomial terms. The a_0-term in Eq. (B.3) has no time dependence, and corresponds to a position shift that is redundant with one of the axle locations. Thus, the analysis uses $a_0 = 0$. Eqs. (B.1) – (B.3) can be combined into a more complete form:

$$\sum_{n=1}^{m} a_n t_{ijk}^{n} \approx x\left(t_{ijk}\right) = x_{ijk} = D_i + A_j + S \times k \,. \tag{B.4}$$

The relevant parts of Eq. (B.4) are the left-most term (polynomial for the vehicle's position as a function of time) and the right-most expression (wheel location), which (B.4) can be simplified to give:

$$\left(\sum_{n=1}^{m} a_n t_{ijk}^{n} \right) - A_j - S \times k \approx D_i \,. \tag{B.5}$$

Equation (B.4) is a system of simultaneous linear equations. The unknown coefficients, $\{a_n, A_j, S\}$, are grouped together on the left-hand side, and must be determined by the analysis. The weigh-pad positions, D_i, are fixed by their interlocking assembly with the spacing pads, as discussed above. For example, measurements by a WIM system with I pads of a vehicle with J axles yields $I \times J$ measurement values of the times, t_{ijk}, for the left-hand side of Eq. (B.5), or twelve values for a six-pad system and a two-axle vehicle. Experience shows that a low-order polynomial (e.g., $n = 3$) is typically adequate. Thus, Eq. (B.5) is an over-determined system, for which an advanced method of solution is required.

A least-squares fitting procedure is appropriate to solve Eq. (B.5) by subtracting the D_i term from both sides, leaving zero on the right-hand side (RHS). Exact equality is not possible for this over-determined system, but near-equality is found by minimizing the function:

$$F = \sum_{ijk} \left[\left(\sum_{n=1}^{m} a_n t_{ijk}^{n} \right) - \left(D_i + A_j + S \times k \right) \right]^2 \,. \tag{B.6}$$

The minimum possible value for F is zero, which is consistent with equality in Eq. (B.5). Minimization of F with respect to a_n corresponds to $\partial F / \partial a_n = 0$, which yields:

$$\sum_{ijk}\left[\left(\sum_{n=1}^{m} a_n t_{ijk}^{n+h}\right) - \left(A_j + S \times k\right) t_{ijk}^{h}\right] = \sum_{ijk} D_i t_{ijk}^{h} \ . \tag{B.7}$$

The RHS is known from the pad locations, D_i, and the pad measurements of the times, t_{ijk}, for the wheel passages. The value of the index, h, has a range from 1 to m. Equation (B.7) expands into three equations for a cubic (third order) fit for the vehicle location, as an example:

$$\sum_{ijk}\left[\left(\sum_{n=1}^{m} a_n t_{ijk}^{n+1}\right) - \left(A_j + S \times k\right) t_{ijk}\right] = \sum_{ijk} D_i t_{ijk} \ . \tag{B.8a}$$

$$\sum_{ijk}\left[\left(\sum_{n=1}^{m} a_n t_{ijk}^{n+2}\right) - \left(A_j + S \times k\right) t_{ijk}^{2}\right] = \sum_{ijk} D_i t_{ijk}^{2} \ . \tag{B.8b}$$

$$\sum_{ijk}\left[\left(\sum_{n=1}^{m} a_n t_{ijk}^{n+3}\right) - \left(A_j + S \times k\right) t_{ijk}^{3}\right] = \sum_{ijk} D_i t_{ijk}^{3} \ . \tag{B.8c}$$

Minimization of F with respect to A_j corresponds to $\partial F/\partial A_j = 0$, which yields:

$$\sum_{ijk}\left[\left(\sum_{n=1}^{m} a_n t_{ijk}^{n}\right) - \left(A_j + S \times k\right)\right] = \sum_{ijk} D_i \ . \tag{B.9}$$

Minimization of F with respect to S corresponds to $\partial F/\partial S = 0$, which yields:

$$\sum_{ijk}\left[\left(\sum_{n=1}^{m} a_n t_{ijk}^{n}\right) - \left(A_j + k\right)\right] = \sum_{ijk} D_i \ . \tag{B.10}$$

This last equation is meaningful only when $k = 1$, allowing simplification to:

$$\sum_{ijk}\left[\left(\sum_{n=1}^{m} a_n t_{ijk}^{n}\right) - \left(A_j + S\right)\right] = \sum_{ijk} D_i \ , \text{ for } k = 1. \tag{B.11}$$

Equation (B.9) has a sum over all the terms with $k = 0$ and $k = 1$, while Eq. (B.11) holds only for $k = 1$. Consequently, Eqs. (B.9) and (B.11) are both included in the linear system of equations that determine the best parameter set. An additional set of equations can be obtained for the vehicle speed, v, by differentiating Eq. B.3:

$$v = \frac{\partial x\left(t_{ijk}\right)}{\partial t} \approx \frac{\partial}{\partial t}\left(\sum_{n=0}^{m} a_n t_{ijk}^{n}\right) = \sum_{n=1}^{m} n\, a_n t_{ijk}^{n-1} \ . \tag{B.12}$$

Equation (B.12) allows estimation of the vehicle speed, v_{ijk}, at each value of time, t_{ijk}. Consequently, Eq. (B.12) also can be rewritten into a function for minimization:

$$G = \sum_{ijk}^{m} \sqrt{v_{ijk} - \sum_{n=1} n\, a_n t_{ijk}^{n-1}} \ . \tag{B.13}$$

Note that Eq. (B.13) is a function of speed and time, but not of the axle spacings, A_j, or of the pad-set shift, S. The polynomial coefficients, a_n, and the speed values, v_{ijk}, are obtained from solving Eq. (B.13). As before, minimization of G requires $\partial G/\partial a_n = 0$, which yields:

$$\sum_{ijk} \left(\sum_{n=1}^{m} n\, a_n t_{ijk}^{n+h-2} \right) = \sum_{ihk} v_{ijk} t_{ijk}^{h-1} \ . \tag{B.14}$$

The value of the index, h, has a range from 1 to m. Equation (B.14) expands into three equations for a cubic (third order) fit for the vehicle speed in this example:

$$\sum_{ijk} \left(\sum_{n=1}^{m} n\, a_n t_{ijk}^{n-1} \right) = \sum_{ihk} v_{ijk} \ . \tag{B.15a}$$

$$\sum_{ijk} \left(\sum_{n=1}^{m} n\, a_n t_{ijk}^{n} \right) = \sum_{ihk} v_{ijk} t_{ijk} \ . \tag{B.15b}$$

$$\sum_{ijk} \left(\sum_{n=1}^{m} n\, a_n t_{ijk}^{n+1} \right) = \sum_{ihk} v_{ijk} t_{ijk}^{2} \ . \tag{B.15c}$$

Equations (B.12)-(B.15) have units of speed, while Eqs. (B.1)-(B.11) have units of distance. Consistent units for all of the equations are needed for a solution, and can be obtained by multiplying both sides of Eqs. (B.15a)-(B.15c) by some time value, τ, which is chosen as $\sum t_{ijk}$ with the sum over all possible values of the set, $\{ijk\}$. Determination of the unknown coefficients, $\{a_n, A_j, S\}$, then is by the simultaneous solution of the Eqs. (B.8), (B.9), (B.11), and (B.15) via standard matrix analysis for the vehicle weight. Two weigh pads do not provide enough data to solve the system of equations using position only [Eqs. (B.8), (B.9), (B.11)] and require the inclusion of the measured speeds [Eqs. (B.15)] as additional input. Adequate data is available to solve these equations for four or more pads (e.g., four, six, and eight weigh pads) using only the position times [Eqs. (B.8), (B.9), (B.11)]. For this situation, only the position information is used to solve for the unknowns and then the speeds are checked for consistency with this solution. This approach in practice produces more meaningful results as the speed measurements can have a much larger error associated with them under certain circumstances.

We next discuss the analysis of measurements from a single weigh pad. A practical matter is the conversion of analog measurements to digital values (A-to-D conversion) with 12 bits of precision, corresponding to 2^{12} (= 4,096) discrete values. The pad-level sensor is calibrated to a maximum of 17,000 pounds. Thus, the digital value is limited by a precision of (17,000 pounds)/(4,096 counts) or roughly 4.2 pounds per count. Each sensor has eight load cells with locations as shown in Fig. B-2. Each load cell has a maximum calibration error of ±50 pounds due to hysteresis and non-linearity. This error corresponds to a typical value of $\sigma_{LOADCELL} \leq 25$ pounds. Then, the net sensor accuracy across all eight of these load cells is $\sigma_{SENSOR} = 8^{1/2} \times \sigma_{LOADCELL} = 71$ pounds (accuracy), which is much larger than the measurement precision (4.2 pounds). However, the major part of the load is distributed over only a few cells, thus reducing the final error. This analysis shows that the weight

measurement is limited by the sensor accuracy (71 pounds), not by the A-to-D precision of 12 bits (4.2 pounds). Consequently, any single-tire weight has a sample standard deviation, $\sigma = 71$ pounds. Any single-axle weight has $\sigma = 2^{1/2}$ x 71 = 100 pounds. The total weight value of J-axle vehicle then has $\sigma = J^{1/2}$ x 100 (e.g., $\sigma = 173$ pounds for a three axle vehicle). In each case, these values of σ arise from the underlying calibration accuracy of the weigh-pad load cells. (In practice distributed loads also fall within the 50 lb error boundary for the entire pad.)

A mico-computer in each weigh pad acquires the data from each load cell, performs the A-to-D conversion at 1,000 times per second (1 kHz), and reports the results to the host computer. The MC12S series 8/16-bit micro-computer for this data acquisition and analysis has a processor speed of 34 MHz. The double arrow in Fig. B-2 indicates the direction of vehicle traversal across the weigh pad. The dashed line in Fig. B-2 indicates the weigh-pad centerline.

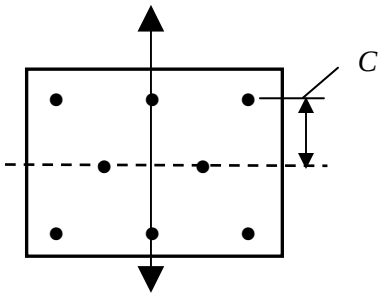

Figure B-2. Locations (●) of eight load cells in each WIM weigh pad (24" x 42").

The weight distribution among the load cells is used to determine the location, X, of the wheel center on the weigh pad, relative to the centerline. Figure B-2 also shows that three load cells are located at $x = +C$ (above the centerline), two lie on the centerline ($x = 0$), and three occur below the centerline at $x = -C$. The g-th load cell measures a weight, $w_g(t)$, at time, t. The total weight of the tire, $W(t)$, on the pad at time, t, is simply the sum of the load cell values:

$$W(t) = \sum_g w_g(t). \tag{B.16}$$

The moment, $X(t)$ of this single-pad weight measurement at time, t, is:

$$X(t) = \left[\sum_g x_g w_g(t)\right] \Big/ W(t). \tag{B.17}$$

Here, the value of x_g is $+C$, 0, or $-C$, depending on the load cell's location in Fig. B-2. (A similar lateral moment is also computed but is only used to check that the tire is fully on the pad.) A linear least-squares fit versus time is used for $X(t)$:

$$X(t) \approx P + Qt. \tag{B.18}$$

The weigh-pad length in the direction of travel is 24". A tire footprint in the direction of travel is typically 12". Consequently, only data from the central 10" – 12" of travel, $-C \le X(t) \le +C$, is used in the fit of Eq. (B.18) to assure that the tire is positioned on the weigh pad. The magnitude, $|Q|$, of the slope from this fit gives an estimate the vehicle's speed, $V = |Q|$. The sign of Q tells the direction of

the vehicle's motion (left side is positive and right negative.) The quality of this fit is measured by the root-mean-squared (RMS) error, ε, between the actual values of tire position, $X(t)$, and the fit, $P + Qt$:

$$\varepsilon = \sqrt{\sum_t \left[X(t) - (P + Qt)\right]^2 \Big/ N} \,. \tag{B.19}$$

The symbol, N, denotes the number of time samples (N~200-400) as the tire traverses the pads. The tire traverses the center, $X = 0$, of i-th pad for the j-th axle on the k-th side at the time, t_{ijk}, which can be obtained from Eq. (B.18) for $X(t_{ijk}) = 0$ as:

$$t_{ijk} = -P/Q \,. \tag{B.20}$$

This time on center, t_{ijk}, is used in the previous analysis of vehicle weight. Moreover, the measurements of total-tire weight, $W(t)$, provide a time-integrated weight from i-th pad for the j-th axle on the k-th side:

$$W_{ijk} = \sum_t W(t) \Big/ N \,. \tag{B.21}$$

The corresponding sample standard deviation in weight, σ_{ijk}, is obtained from the equation:

$$\sigma_{ijk} = \sqrt{\sum_t \left[W(t) - W_{ijk}\right]^2 \Big/ (N-1)} \,. \tag{B.22}$$

Clearly, these results are obtained over the same center section of the pad as the moment to assure that the tire is fully on the pad. The results of this analysis from the i-th pad for the j-th axle on the k-th side are: (1) the vehicle speed, V, from the fit of Eq. (B.18); (2) the RMS error, ε, of the position-versus-time fit from Eq. (B.19); (3) the time on center, t_{ijk}, from Eq. (B.20); (4) the time-averaged weight, W_{ijk}, from Eq. (B.21); and (5) the corresponding estimate of the sample standard deviation in weight, σ_W, from Eq. (B.22). This analysis allows comparison of the vehicle speed, V, from the pad-level fit of Eq. (B.18) to the vehicle-level fit of speed, v, from Eq. (B.12). Moreover, an excess value of the RMS fitting error, ε, from Eq. (B.19) typically indicates that the particular run is flawed, and needs to be re-measured.

After a tire traverses the a pad, the micro-computer reports these pad-level results to the host computer, which combines them as follows. The weight from the i-th pad for the j-th axle is a sum of the tire weights on both sides ($\sum_k$). The average weight, W_j, of the j-th axle across all of the weigh pads then is:

$$W_j = \sum_{k=0}^{1} \sum_{i=1}^{I} W_{ijk} \Big/ I \,. \tag{B.23}$$

Here, the symbol, I, denotes the number of pad pairs (e.g., $I = 3$ for 6 weigh pads). The corresponding sample standard deviation is:

$$\sigma_j = \sqrt{\sum_{k=0}^{1} \sum_{i=1}^{I} \sigma_{ijk}^2} \,. \tag{B.24}$$

The total vehicle weight, W_{TOT}, is simply the sum of the axle weights:

$$W_{TOT} = \sum_{j=1}^{J} W_j \,. \tag{B.25}$$

Here, the symbol, J, denotes the number of axles, as before. The corresponding sample standard deviation, σ_W, in the total vehicle weight in a 2-pad system is:

$$\sigma_W = \sqrt{\sum_{j=1}^{J} \sigma_j^2} \,. \tag{B.26a}$$

For a larger system, we have multiple measurements for each tire weight. With these systems the standard deviation is obtained from the root-mean-square of the tire weights:

$$E_W = B\sqrt{\sum_{k=0}^{1}\sum_{j=1}^{I}\sum_{j=1}^{J}\left(W_{ijk} - W_j\right)^2} \,. \tag{B.26b}$$

As before, I denotes the number of pad pairs, and J is the number of vehicle axles. B is the correction factor for a Student's T-distribution for a 95% confidence interval.

The results of the vehicle- and pad-level analyses are reported to the user by the host computer, as summarized in Table B.1. The default value for the error flags in Table B.1 is zero. If any of the limits in Table B.1 are exceeded (e.g., vehicle speed too fast), then the error flag in Table B.1 is set to 1 to flag the run as potentially "bad." Specifically, Table B.1 shows details of the filtering limits. At the client level (above the Host), the vehicle type is known. A corresponding table of limit values can be stored by vehicle type, thus providing consistency in the filtering process. These limits have been determined empirically from tests at Ft. Lewis during 2006 and subsequently refined further. The user can accept or ignore these error flags for final results. The limits in Table B.1 use two additional parameters that relate to those above. One is the average over the differences between the actual and fitted distances from Eq. (B.6):

$$K = \sum\left[\left(\sum_{n=1}^{m} a_n t_{ijk}^n\right) - \left(D_i + S \times k\right)\right] \Big/ \left(I \times J\right). \tag{B.27}$$

The second is the average over differences between the actual and fitted speeds from Eq. (B.13):

$$G = \sum_{ijk}^{m}\left(v_{ijk} - \sum_{n=1} n\, a_n t_{ijk}^{n-1}\right) \Big/ \left(I \times J\right). \tag{B.28}$$

Table B-1. Summary of WIM results

Variable Name	Brief description of meaning	Equation for constraint
BadDistFit	average distance of actual from fit	$K > 0.001$"
BadSpdFit	average speed of actual from fit	$L > 0.20$ mph
BadDistRms	RMS of distance to actual fit	$[F/(I*J)]^{1/2} > 0.50$"
BadSpdRms	RMS of speed to actual fit	$[G/(I*J)]^{1/2} > 0.30$ mph
BadFitRms	combined above two	$[(F+G)/(I*J)]^{1/2} > 0.75$
BadTooFast	upper speed limit	$V > 5.0$ mph
BadTooSlow	lower speed limit	$V < 0.2$ mph
BadSpdDelt	min/max speed difference	$V_{max} - V_{min} > 0.7$ mph
BadStdWt	variation of weight between pads	$\varepsilon > 1\%$ for 2-pads; $E > 5\%$ for ≥ 4 pads
BadAveWt	bad average weight reported from pad	bad A-to-D (e.g., over-/under-flow)
BadCell	flag for bad load cell reading	over-/under-flow from loadcell
BadPadCt	odd number of operational pads	odd number of pads reporting
BadAxlPn	axle spacing too small	$\lvert A_j - A_{j\pm1}\rvert < 10.0$"
MissingAxleData	missing data from pads	$J <$ known axle number for each pad
AxleTimeOut	fewer axles than requested	$J =$ same for all pads, but less than expected

INTERNAL DISTRIBUTION

1. R. K. Abercrombie
2. L. M. Hively
3. M. B. Scudiere
4. F. T. Sheldon
5. J. P. Trien
6. B. A. Worley
7. Central Research Library
8. ORNL Laboratory Records-RC
9. ORNL Laboratory Records-Office of Technical Information and Classification (OSTI)